Cretaceous and Triassic subduction-accretion, high-pressure–low-temperature metamorphism, and continental growth in the Central Pontides, Turkey

A.I. Okay[†]
O. Tüysüz[‡]
Istanbul Teknik Üniversitesi, Avrasya Yerbilimleri Enstitüsü, Maslak, Istanbul 34469, Turkey

M. Satır[§]
Institut für Geowissenschaften, Universität Tübingen, Wilhelmstraße 56, D-72074 Tübingen, Germany

S. Özkan-Altıner[#]
D. Altıner[††]
Middle East Technical University, Department of Geology, Ankara 06531, Turkey

S. Sherlock[‡‡]
Department of Earth Sciences, Open University, Walton Hall, Milton Keynes MK7 6AA, UK

R.H. Eren
Anadolu Yerbilimleri Ltd. Şirketi, Perpa Ticaret Merkezi, No. 1955, Okmeydanı, Istanbul, Turkey

ABSTRACT

Biostratigraphic, isotopic, and petrologic data from the Central Pontides document major southward growth of the Eurasian continental crust by subduction-accretion during the Cretaceous and Triassic Periods. A major part of the accreted material is represented by a crustal slice, 75 km long and up to 11 km thick, consisting of metabasite, metaophiolite, and mica schist that represent underplated Tethyan oceanic crustal and mantle rocks. They were metamorphosed at 490 °C and 17 kbar in mid-Cretaceous time (ca. 105 Ma). The syn-subduction exhumation occurred in a thrust sheet bounded by a greenschist facies shear zone with a normal sense of movement at the top and a thrust fault at the base. A flexural foreland basin developed in front of the south-vergent high-pressure–low-temperature (HP-LT) metamorphic thrust sheet; the biostratigraphy of the foreland basin constrains the exhumation of the HP-LT rocks to the Turonian–Coniacian, ~20 m.y. after the HP-LT metamorphism, and ~25 m.y. before the terminal Paleocene continental collision. The Cretaceous subduction-accretion complex is tectonically overlain in the north by oceanic crustal rocks accreted to the southern margin of Eurasia during the latest Triassic–earliest Jurassic. The Triassic subduction-accretion complex is made up of metavolcanic rocks of ensimatic arc origin and has undergone a high pressure, greenschist facies metamorphism with growth of sodic amphibole. Most of the Central Pontides consists of accreted Phanerozoic oceanic crustal material, and hence is comparable to regions such as the Klamath Mountains in the northwestern United States or to the Altaids in Central Asia.

Keywords: Pontides, Turkey, HP-LT metamorphism, exhumation, continental growth, orogeny.

INTRODUCTION

The Pacific mountain belts along the western North American margin have grown oceanward by subduction-accretion and by incorporation of oceanic edifices, such as island arcs, oceanic islands, and oceanic plateaus (e.g., Coney et al., 1980; Irwin, 1981; Ernst, 1984). In contrast, the Alpine-Himalayan orogen is generally considered the result of the collision of the megacontinents Laurasia, Gondwana, India, and a small number of continental terranes during the Tertiary (e.g., Dercourt et al., 1986; Şengör, 1987).

Here we show extensive precollisional growth of continental crust along the southern margin of Laurasia in the Central Pontides by accretion and underplating of oceanic rocks in the Late Triassic and Late Cretaceous.

A second aim of the paper is to contribute to the evaluation of the mechanism of exhumation of high-pressure–low-temperature (HP-LT) metamorphic rocks. Most HP-LT metamorphic complexes occur within the crystalline part of the orogen associated with ophiolites and other metamorphic rocks. In contrast, those in the Central Pontides in northern Turkey are closely associated with sedimentary sequences with ages that overlap the age of the HP-LT metamorphism. Interpretation of the new isotopic, biostratigraphic, and structural data indicates that the HP-LT metamorphic rocks from the Central Pontides were exhumed in a forearc setting during the ongoing oceanic subduction.

A third aim of the paper is to contribute to the regional tectonics of the Tethyan region. Geological data from the Central Pontides have been important in models regarding the evolution of the Paleo-Tethys (Şengör et al., 1984; Şengör, 1984; Yılmaz and Şengör, 1985;

[†]E-mail: okay@itu.edu.tr.
[‡]E-mail: tuysuz@itu.edu.tr.
[§]E-mail: satir@uni-tuebingen.de.
[#]E-mail: altiner@metu.edu.tr.
[††]E-mail: demir@metu.edu.tr.
[‡‡]E-mail: s.sherlock@open.ac.uk.

GSA Bulletin; September/October 2006; v. 118; no. 9/10; p. 1247–1269; doi: 10.1130/B25938.1; 14 figures; 4 tables.

Tüysüz, 1990; Ustaömer and Robertson, 1994, 1997; Yılmaz et al., 1997; Robertson et al., 2004). A major part of the oceanic assemblages in the Central Pontides, interpreted in the past to be Triassic or older, is shown here to be of Cretaceous age. This requires a reevaluation of the Paleo- and Neo-Tethyan history of the Pontides, and their relation to the opening of the Black Sea, a potential hydrocarbon-bearing basin.

TECTONIC SETTING

The term *Central Pontides* is a geographical term for the arched central part of the Pontide orogenic belt (Fig. 1). It lies between the İzmir-Ankara suture in the south and the Black Sea in the north. The latter is a backarc basin, which opened during the Cretaceous above the northward-subducting Tethyan ocean (e.g., Boccaletti et al., 1974; Görür, 1988). The Central Pontides includes two Pontide terranes: the Istanbul and Sakarya zones (Fig. 1). The Istanbul zone is characterized by an Ordovician to Carboniferous sedimentary succession of passive margin type unconformably overlain by Triassic and younger rocks (e.g., Görür et al., 1997). In contrast, the Sakarya zone has a basement of Permo-Triassic subduction-accretion complexes unconformably overlain by a Jurassic and younger sedimentary cover (e.g., Okay and Tüysüz, 1999; Robertson et al., 2004; Okay and Göncüoğlu, 2004). In the Central Pontides the tectonic juxtaposition of these two zones occurred during the early Late Cretaceous (Cenomanian–Turonian) (Tüysüz, 1999).

A major part of the Central Pontides consists of metamorphic rocks, known as the Kargı Massif, occupying an area of 55 km to 120 km, and generally regarded as part of the Sakarya zone (Fig. 2). The Kargı Massif is made up of northwest-dipping, crustal-scale tectonic slices separated by Cretaceous and younger thrust faults (Tüysüz, 1990, 1993; Yılmaz et al., 1997; Ustaömer and Robertson, 1997, 1999). Previous studies consider the Kargı Massif to be a Paleo-Tethyan subduction complex consisting of accreted pre-Jurassic ophiolite, mélange, and magmatic arc sequences. Our field and isotopic data show the presence of a crustal-scale

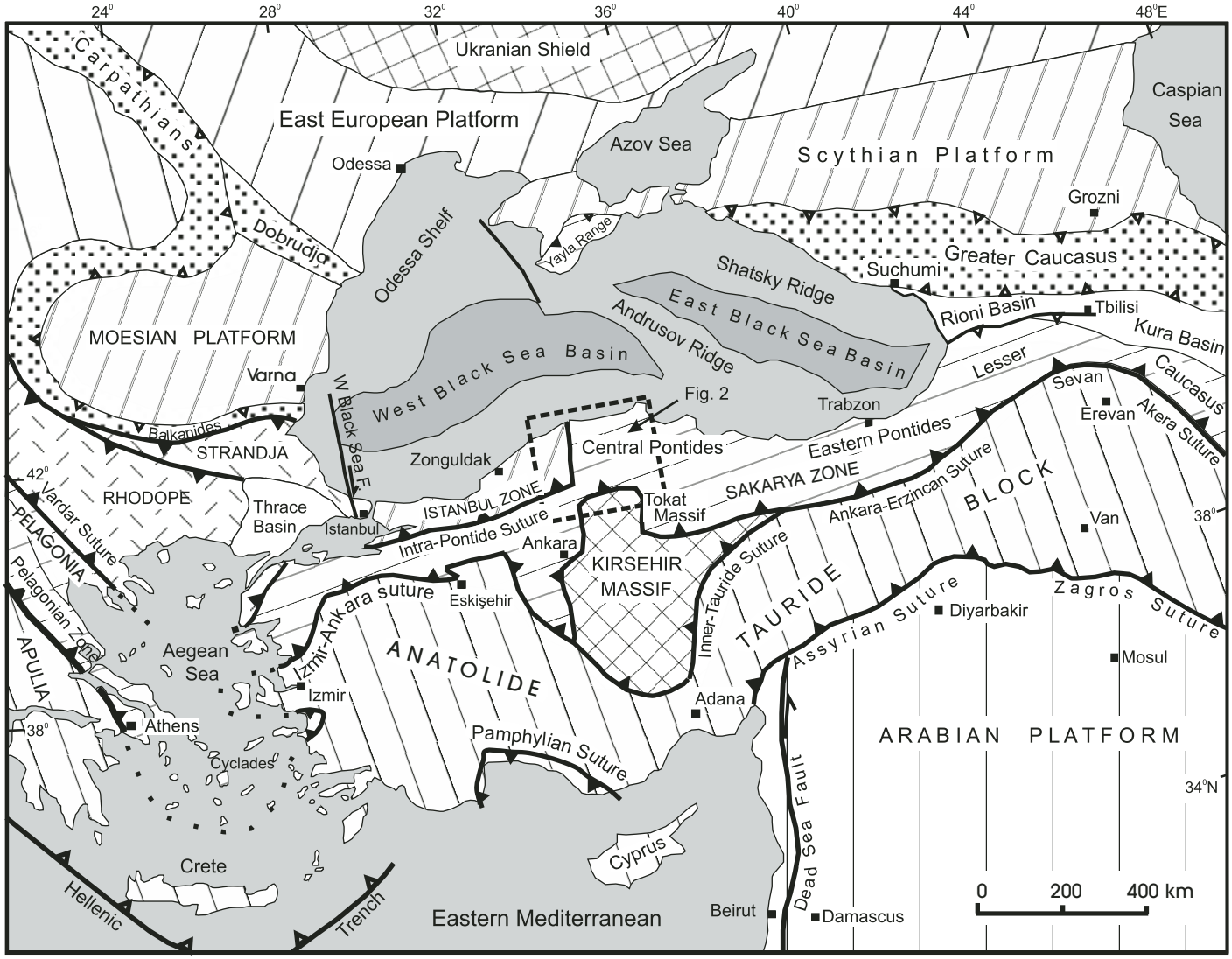

Figure 1. Tectonic map of the Eastern Mediterranean region (modified from Okay and Tüysüz, 1999). Dashed-line box shows location of Figure 2.

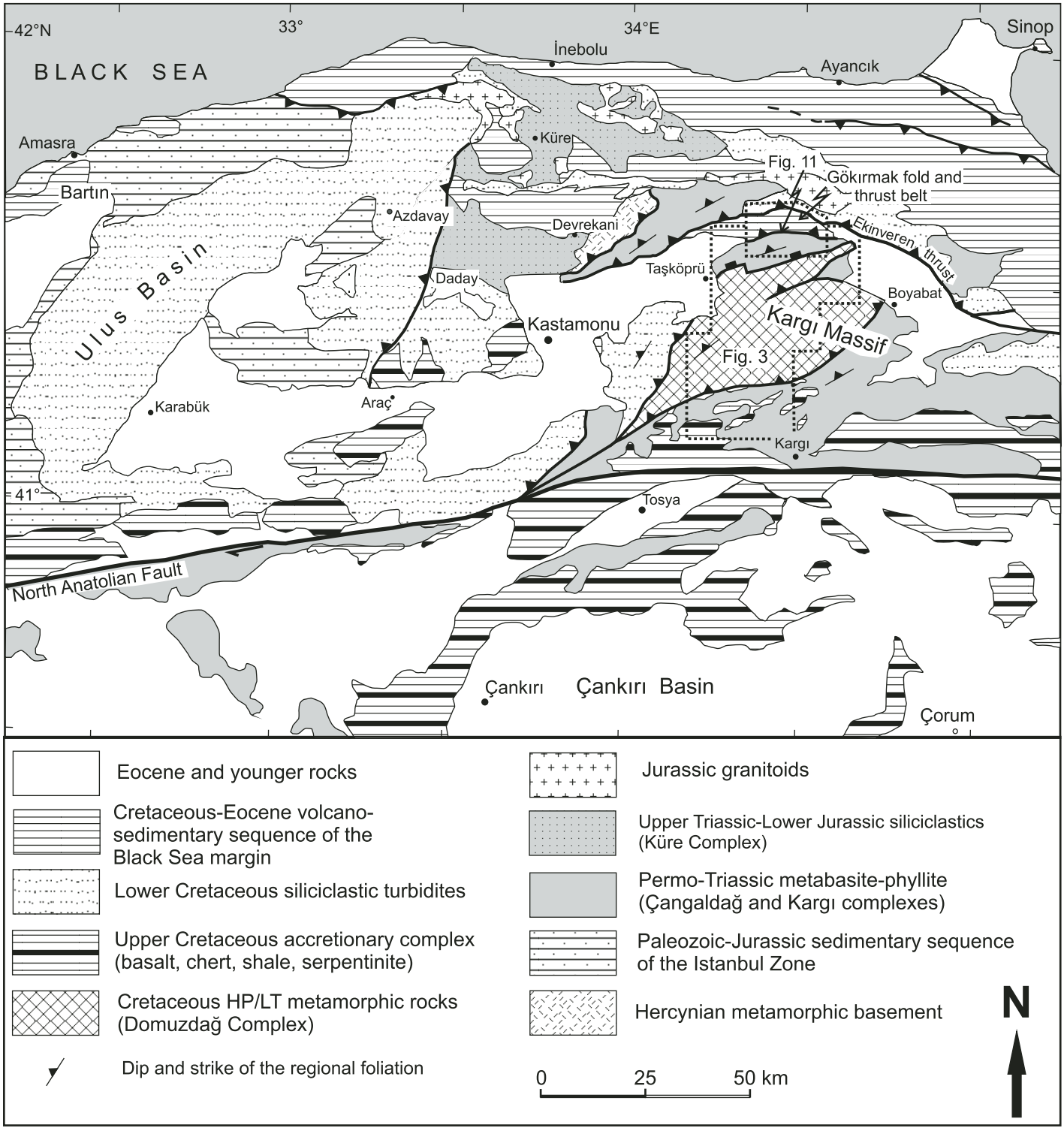

Figure 2. Tectonic map of the Central Pontides (compiled from Tüysüz, 1998; Uğuz et al., 2002; Aksay et al., 2002; and this study). Dashed-line boxes show locations of Figures 3 and 11.

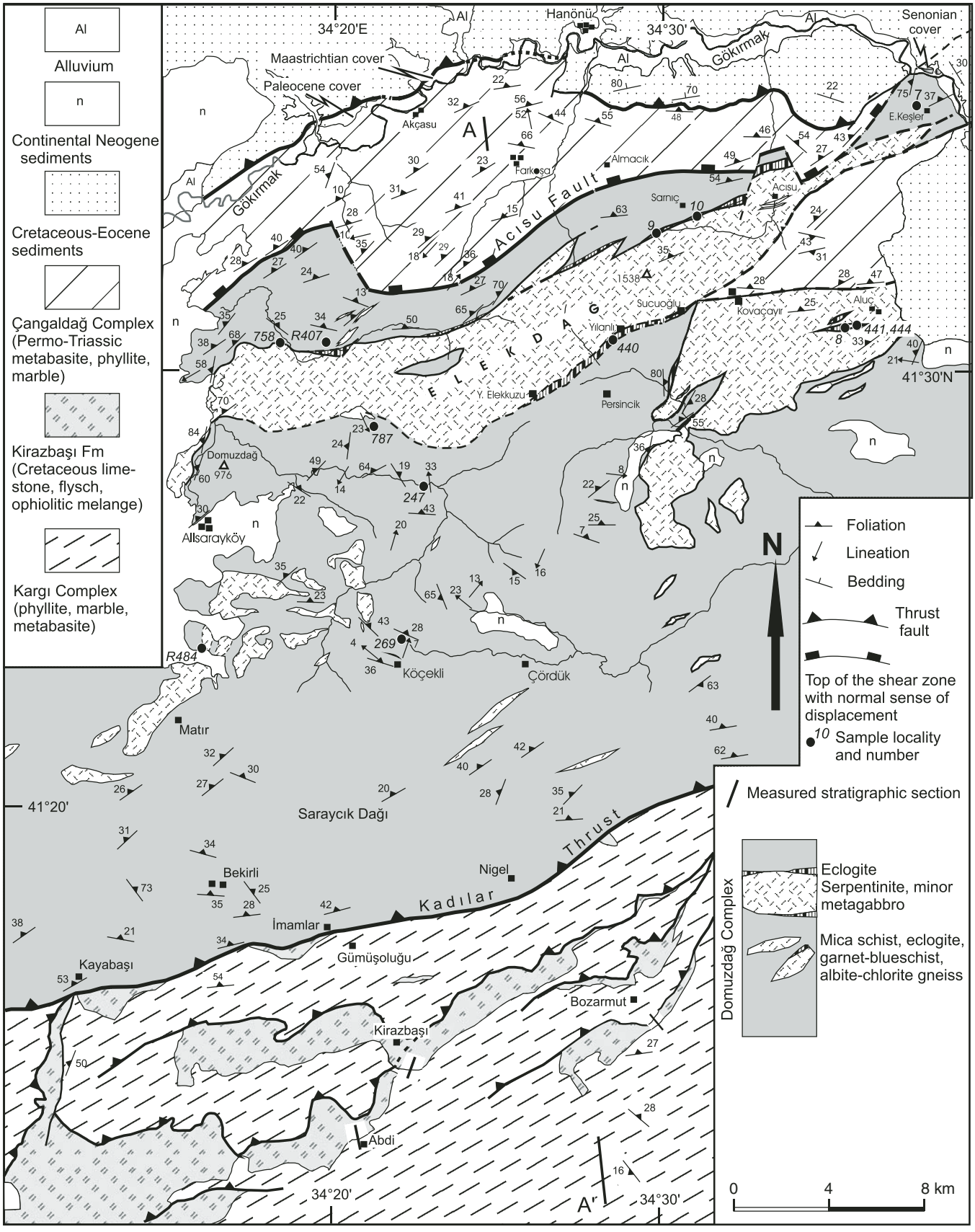

Figure 3. Geological map of the central portion of Kargı Massif, based on Eren (1979), Tüysüz (1985), and this study. For location, see Figure 2.

Cretaceous HP-LT metamorphic unit in the center of the Kargı Massif (Fig. 2).

CRETACEOUS HP-LT METAMORPHIC SLICE: THE DOMUZDAĞ COMPLEX

The Domuzdağ Complex forms a northwest-dipping crustal slice, 75 km long and up to 11 km thick, extending in a northeast-southwest direction and bisecting the Kargı Massif (Fig. 2). It is tectonically overlain by Permo-Triassic metabasite and phyllite in the north and by a slightly metamorphosed Cretaceous flysch sequence in the west. In the south it is underlain by a Late Cretaceous foreland basin and by the metamorphic rocks of the Kargı Complex (Figs. 3 and 4).

The Domuzdağ Complex is a complexly deformed, structurally thickened but coherent tectonic package with a pervasive penetrative foliation. It is made up of quartz–mica schist (~60% of the outcrops), metabasite (~25%), minor marble and metachert (~3%), and irregular tectonic lenses of metamorphosed ophiolite represented mainly by serpentinite (~12% of the outcrops). There are no data on the protolith ages of the Domuzdağ Complex. Metabasites in the Domuzdağ Complex range from eclogite through garnet-blueschist to albite-chlorite gneiss, depending on the degree of retrogression. Metabasites and metaophiolite fragments dominate the upper parts of the Domuzdağ Complex in the north, where they make up >70% of the outcrops, whereas quartz–mica schists are the main rock type in the basal parts of the complex in the south. In previous studies the southern part of the Domuzdağ Complex was assigned to a different unit (the Bekirli Formation of Tüysüz and Yiğitbaş, 1994; Domuzdağ-Saraycıkdağ Complex of Ustaömer and Robertson, 1997). However, the northern and southern parts of the Domuzdağ Complex share a common metamorphic and structural history, and the southward change in lithology is gradual.

Two generations of penetrative foliation can be recognized in the Domuzdağ Complex. A steeply dipping first generation of foliation associated with isoclinal folds, probably coeval with the HP-LT metamorphism, is preserved in the north near the Elekdağ lherzolite. The S1 foliation is overprinted toward the south by a shallower dipping second generation of foliation associated with tight recumbent folds. The intersection of S1 and S2 has produced an intersection lineation parallel to the S2 fold axis. The dips of S1 and S2 are generally to the north (Fig. 5). The shallowly dipping lineation shows a high scatter in its trend, indicating subsequent refolding.

The oldest sedimentary rocks that lie unconformably over the Domuzdağ Complex are latest Santonian–earliest Campanian pelagic limestones. They are observed in a small locality in the northeast, north of the village of Keşler (Fig. 3), where a basal conglomerate 10 m thick, with clasts of metamorphic rocks, passes up through a 2-m-thick sandstone layer into pelagic

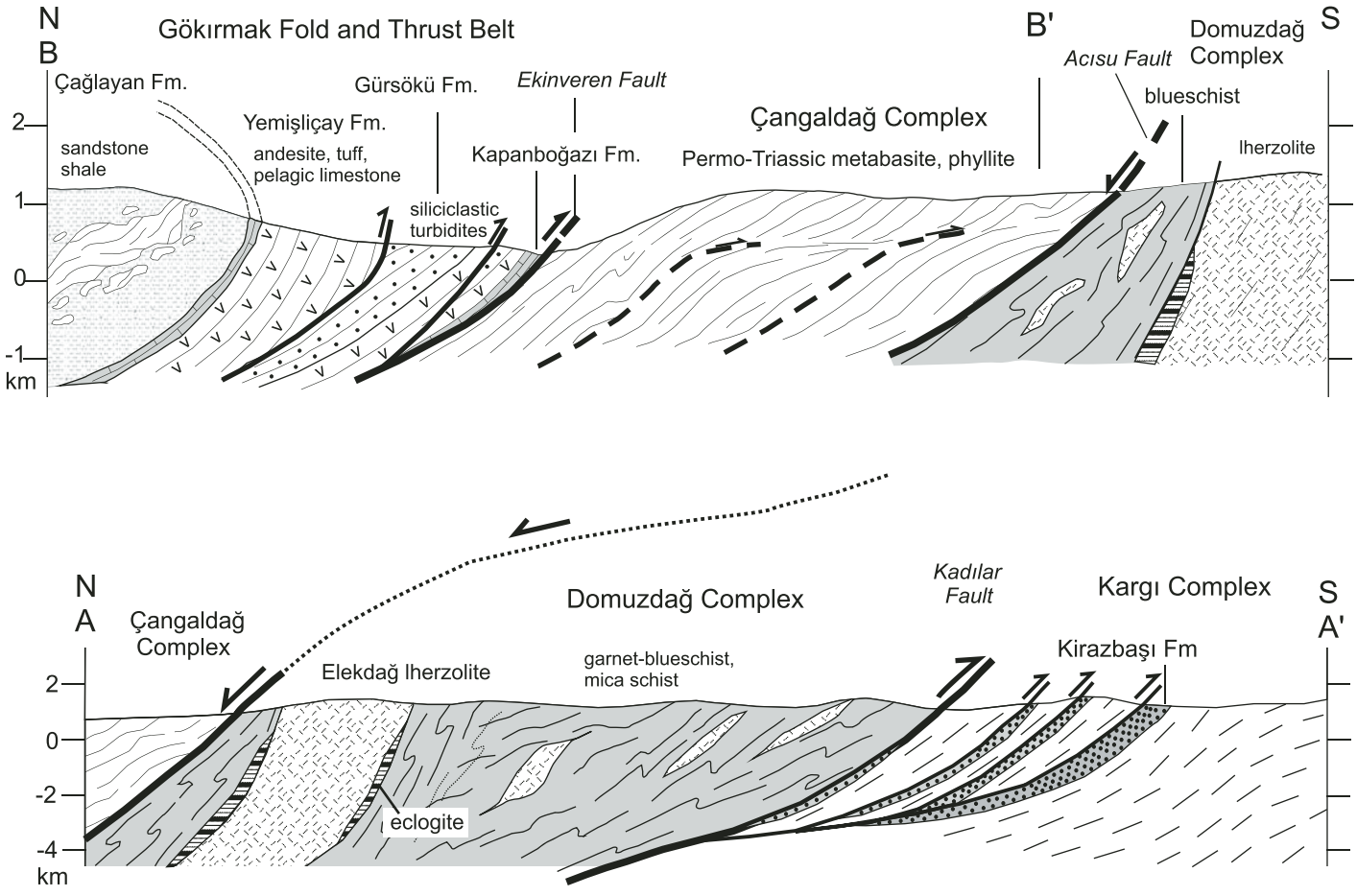

Figure 4. Geological cross sections across the Central Pontides, illustrating the tectonic setting of the HP-LT metamorphic slice. For location of cross-section A–A′, see Figure 3, and for cross-section B–B′, Figure 11. Note the difference in scale between the two cross sections.

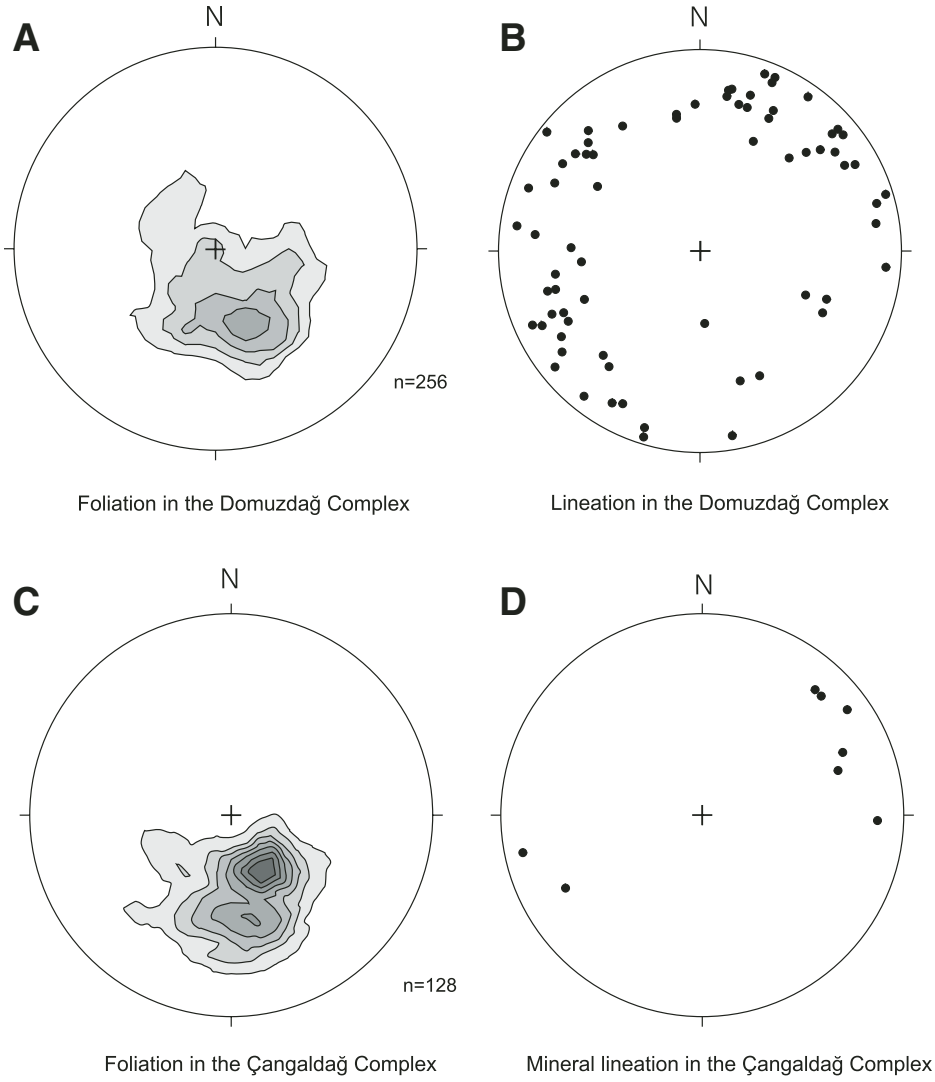

Figure 5. Lower hemisphere equal-area projections of foliation and lineation in the Domuzdağ (A and B) and Çangaldağ (C and D) complexes. Contours are at 2, 4, 6, 8, 10, 12, and 14% per 1% area.

limestones ~40 m thick with *Globotruncana arca* (Cushman), *G. linneiana* (d'Orbigny), *G. bulloides* Vogler, *Globotruncanita elevata* (Brotzen), and *Marginotruncana coronata* (Bolli). At several localities, nummulite-bearing neritic limestones of early–middle Eocene age lie unconformably over the metamorphic rocks of the Domuzdağ Complex.

The geochemistry of the metabasic rocks from the Domuzdağ Complex was studied by Ustaömer and Robertson (1999). On the basis of whole and trace element analyses from 28 metabasite samples, they interpret the metabasic rocks in the Domuzdağ Complex as mid-ocean-ridge (MORB) type basalts. This is supported by the trace element geochemistry of an eclogite studied by Altherr et al. (2004).

Ophiolite Fragments within the Domuzdağ Complex

The metamorphic rocks of the Domuzdağ Complex comprise tectonic blocks of ultramafic rock and gabbro ranging from a few meters up to several tens of kilometers in length. These ophiolites, as used in the broader sense of the term, can be compared to the Franciscan-type ophiolites of Dilek (2003). The contacts of the ultramafic bodies are parallel to the penetrative foliation in the host schists and metabasites. The largest of the ultramafic bodies is the Elekdağ lherzolite, 35 km long and up to 3 km wide, which forms an ENE-trending ridge (Fig. 3). In previous studies the Elekdağ lherzolite was regarded as a different unit from the Domuzdağ Complex (Eren, 1979; Tüysüz, 1990; Ustaömer and Robertson, 1997, 1999). However, apart from its larger size, it is similar to the other ultramafic lenses in the Domuzdağ Complex, and our geological mapping reveals that it is totally enclosed by the HP-LT metamorphic rocks (Fig. 3). The Elekdağ lherzolite shows a tectonite fabric and consists of olivine with lesser amounts of ortho- and clinopyroxene and Cr-spinel. Ortho- and clinopyroxene occur in roughly equal amounts, ~10–15 modal% each. In several samples, olivine is partially replaced by Ti-clinohumite. Titanoclinohumite, which is compositionally similar to olivine but contains titanium, fluorine, and hydroxyl, is described from several HP and ultrahigh-pressure (UHP) ultramafic rocks (e.g., Aoki et al., 1976; Evans and Trommsdorff, 1983; Okay, 1994). The Elekdağ lherzolite is partially to completely serpentinized. Antigorite is the main serpentine mineral, which has replaced 40–100% of the peridotite. The smaller ultramafic bodies in the Domuzdağ Complex consist of antigorite with rare relics of clinopyroxene.

Metagabbro lenses with a maximum thickness of a few hundred meters occur on the margins or within the Elekdağ lherzolite, or within the smaller serpentinite lenses in the schists (Eren, 1979). The metagabbro lenses consist of calcic and sodic amphibole, clinozoisite, chlorite, and garnet.

Petrology

The HP-LT metamorphic rocks from the Central Pontides have been known since the time of Milch (1907) and were studied petrographically by Eren (1979). However, there had been no petrological study of these rocks except for a recent description of a single lawsonite-tourmaline–bearing eclogite from Elekdağ (Altherr et al., 2004). Our study of the petrology of the Domuzdağ Complex is based on petrographical reexamination of >600 thin sections from the collection of Eren (1979) and Tüysüz (1985), as well as >100 new petrographic sections.

The metabasic rocks in the Domuzdağ Complex range from eclogite through garnet-blueschist to albite-epidote-chlorite gneiss. The degree of greenschist facies overprint increases southward toward the lower parts of the Domuzdağ Complex. However, a common lithostratigraphy and the presence of HP-LT metamorphic relicts, even in the southernmost outcrops of the Domuzdağ Complex (Fig. 6), indicate that all rocks of the Domuzdağ Complex have undergone an initial HP-LT regional metamorphism. However, because of the strong greenschist facies overprint, it is not clear whether the Domuzdağ Complex records

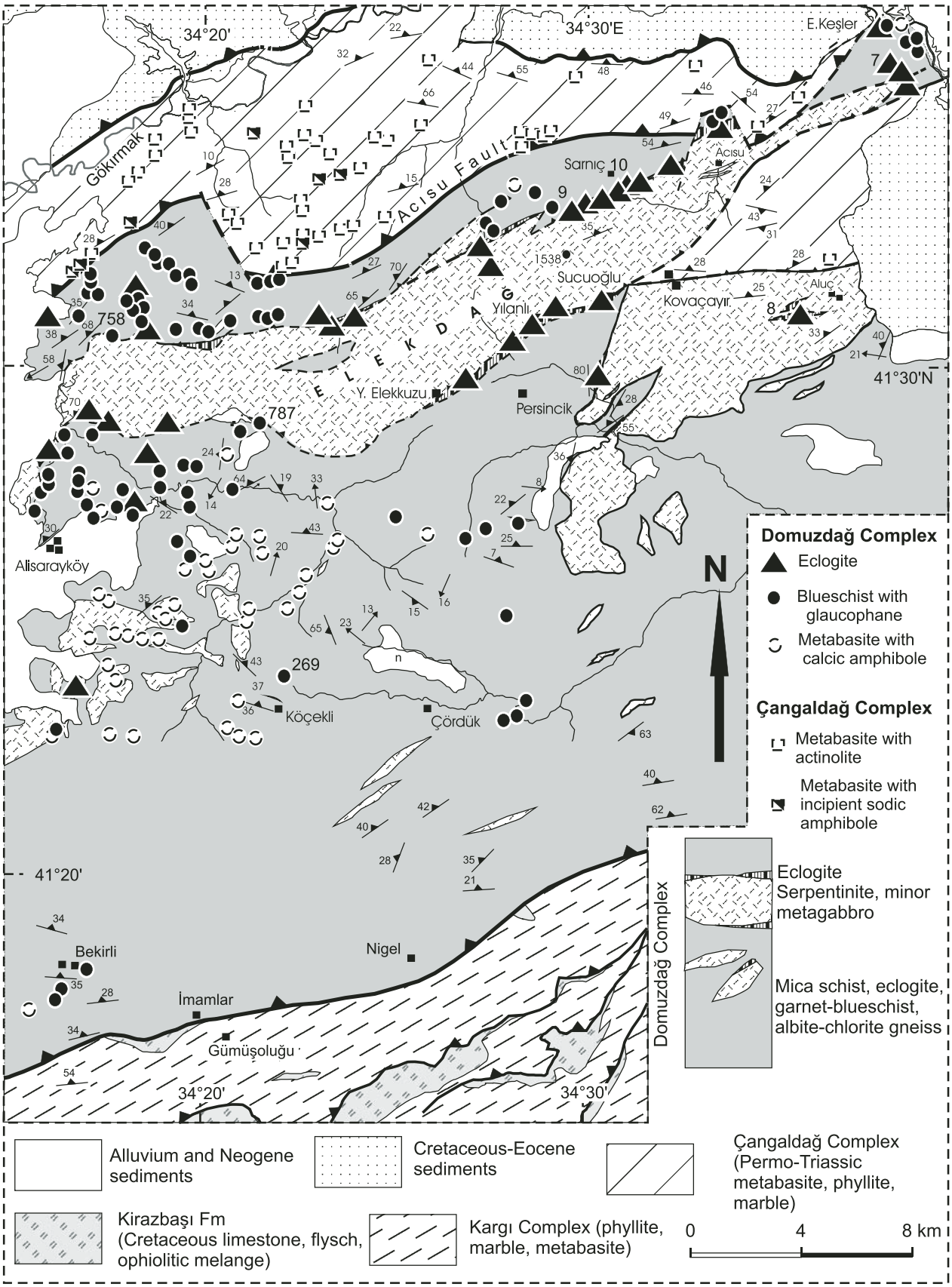

Figure 6. Geological map of the Domuzdağ Complex, showing the distribution of extant blueschists on the basis of the petrography of >600 samples.

a coherent and single HP-LT metamorphic evolution or whether there are accreted tectonic slices with different HP-LT metamorphic histories.

The spatial distribution of the garnet-blueschists and albite-epidote-chlorite gneisses (Fig. 6) and their field relations indicate that they are related by the varying degrees of greenschist facies overprint. On the other hand, eclogites are generally found in bands, up to several hundred meters thick and several kilometers long, along the margins or within the Elekdağ lherzolite (Figs. 3 and 4). The eclogite bands also contain subordinate quartz–mica schist layers. This observation, and rare eclogite boudins within the mica schists, suggest that eclogites are not exotic tectonic lenses but are cogenetic with the rest of the HP-LT metamorphic rocks. The lack of retrogression in proximity to the ultramafic rocks is probably related to the selective absorption of the incoming fluids for serpentinization, leaving eclogites dry during the exhumation. Mica schists with the best preserved HP mineral assemblages also lie along the ultramafic rock contacts.

The common mineral assemblage in the eclogites is garnet + omphacite + glaucophane + epidote + white mica. The texture of the eclogites ranges from granoblastic to porphyroblastic. Typically, idioblastic garnet poikiloblasts, 1–4 mm across, are set on an oriented matrix of omphacite, glaucophane, and mica. Garnet contains inclusions of omphacite, clinozoisite, lawsonite, mica, quartz, and rutile (Fig. 7A). Garnet-blueschists, differentiated from the eclogites by the absence of omphacite, are common, especially north and southwest of the Elekdağ lherzolite (Fig. 6). The typical mineral assemblage in the garnet-blueschists is garnet + glaucophane + epidote + chlorite + white mica ± quartz. With an increase in the greenschist facies overprint, the sodic amphibole and garnet are partially to completely replaced by chlorite, albite, and calcic amphibole, and the rock grades into an albite-epidote gneiss with the

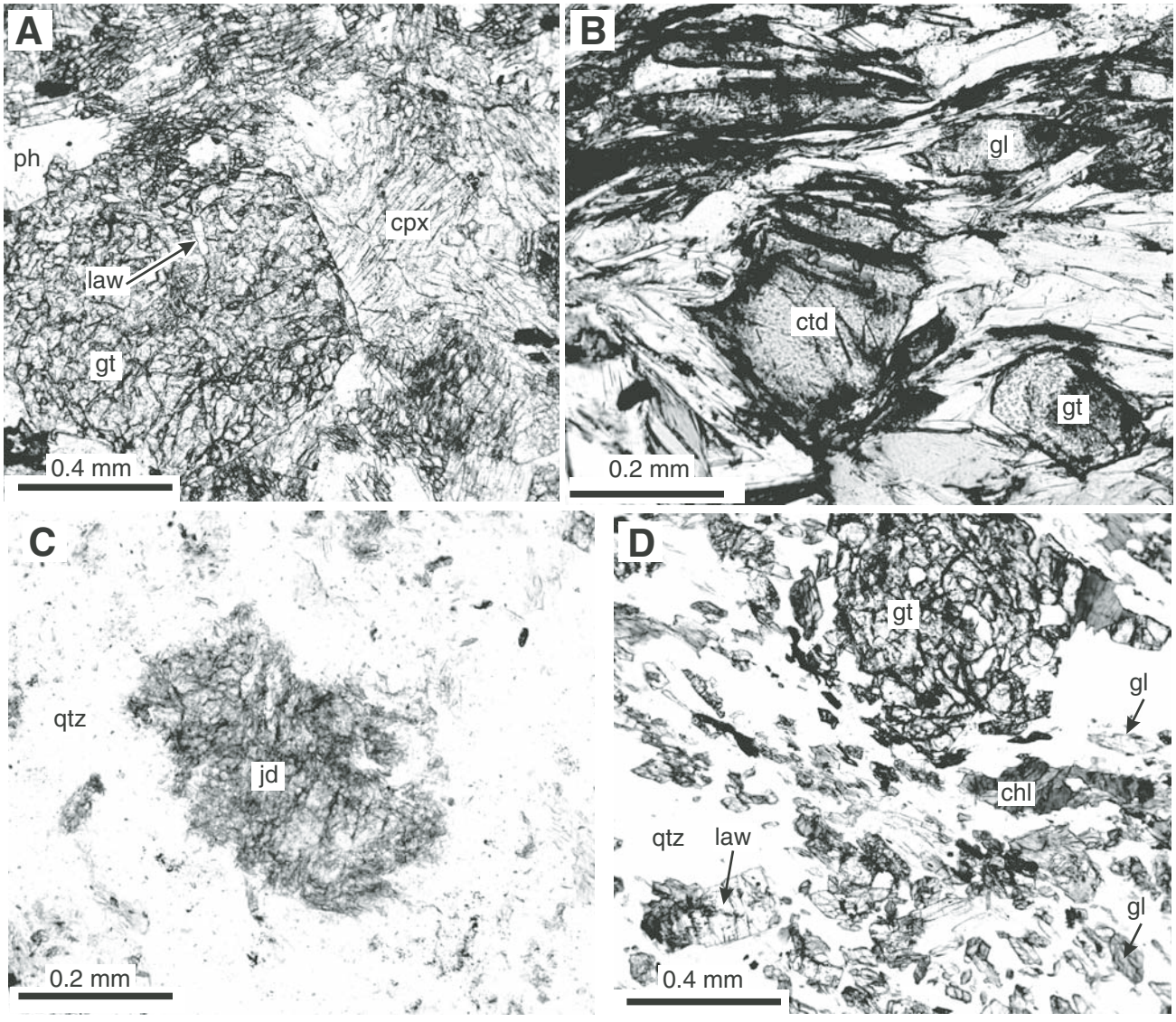

Figure 7. Photomicrographs from the Domuzdağ Complex. (A) Eclogite (10B) with garnet (gt), omphacite (cpx), and phengite (ph). Garnet contains inclusions of lawsonite (law). (B) Mica schist (758B) with chloritoid (ctd), glaucophane (gl), and garnet (gt). (C) Jadeite fels (R484) with jadeite (jd) and quartz (qtz). (D) Mica schist (R259) with garnet (gt), lawsonite (law), glaucophane (gl), chlorite (chl), and quartz (qtz).

mineral assemblage albite + epidote + chlorite + actinolite-hornblende + white mica.

The HP-LT metamorphic minerals are rarely preserved in the mica schists, in which the common mineral assemblage is quartz + white mica ± chloritoid ± garnet ± clinozoisite ± albite. However, at a few localities the petrogenetically important mineral assemblage quartz + white mica + chloritoid + glaucophane + garnet was found (Fig. 7B). Jadeite, partially replaced by albite and coexisting with quartz and white mica, is observed in one sample (Fig. 7C, R484). The common mineral assemblage in the metacherts is quartz + garnet + sodic amphibole + white mica ± epidote. Lawsonite as a matrix mineral was found in one sample (R407), possibly a former siliceous shale, where it occurs along with garnet, sodic amphibole, quartz, and epidote (Fig. 7D).

Mineral Chemistry

Four eclogites and three chloritoid-glaucophane mica schists were analyzed with a Camebax SX-50 electron microprobe at Ruhr University Bochum to constrain the pressure-temperature (P-T) evolution of the Domuzdağ Complex. Operating conditions were 15 kV accelerating voltage, 10 NA beam current, and a beam size 8 ηm for the micas and 2 ηm for the other minerals. The estimated modes and representative mineral compositions are given in Tables 1 and 2, respectively. Garnets from the eclogites are essentially almandine-grossular solid solutions with minor pyrope (3–12 mol%) and spessartine (1–8 mol%) end members (Fig. 8A). These garnets exhibit minor prograde zoning with a slight increase in Mg and Fe/Mg ratio and a decrease in Mn toward the rim. Garnets from the chloritoid-glaucophane mica schists are almandine-spessartine-grossular solid solutions with minor pyrope end members (0–6 mol%). Garnets from chloritoid-glaucophane mica schist sample 758B show a strong growth zoning with a sharp decrease in Mn and an increase in Fe and Mg toward the rim (Table 2). Sodic pyroxene in the eclogites is omphacite in composition (Fig. 8B), except in sample 7, in which jadeite cores are rimmed by omphacite, attesting to the immiscibility gap between these compositions (e.g., Carpenter, 1980). Sodic amphibole from the eclogites is glaucophane, and, from the mica schists, ferroglaucophane in composition (Fig. 8C). In sample 8A the sodic amphibole is partially replaced by colorless actinolite. Phengite with 3.32–3.49 Si per formula unit (Fig. 8D) is closely associated with paragonite. In the chloritoid-glaucophane schists the amount of phengite and paragonite in the rock is approximately equal. Paragonite compositions are very close to that of the end-member paragonite, with only minor K substitution (<0.7 wt%) (Table 2). Epidotes with Fe/(Fe + Al) ratios of 0.13–0.21 are minor constituents of the eclogites. In eclogite sample 8A, clinozoisite with an Fe/(Fe + Al) ratio of 0.03–0.05 is partially replaced by epidote with an Fe/(Fe + Al) ratio of 0.13. Lawsonite occurs in three of the analyzed eclogites as small inclusions in garnet, as reported by Altherr et al. (2004).

TABLE 1. ESTIMATED MODAL AMOUNTS OF THE ANALYZED HP-LT METAMORPHIC ROCKS FROM THE DOMUZDAĞ COMPLEX

	Eclogite				Chloritoid-glaucophane mica schist		
Sample no.	7	8A	9C	10B	269	758B	787
Garnet	6	28	29	36	2	16	–
Omphacite	32	22	27	45	–	–	–
Sodic amphibole	7	24	30	–	3	4	8
Chloritoid	–	–	–	–	19	14	10
Lawsonite	–	tr	tr	tr	–	–	–
Clinozoisite	–	3	–	–	–	–	–
Epidote	2	10	6	3	–	–	–
White mica	29_{pa}	–	2_{ph}	$4_{ph,pa}$	$34_{ph, pa}$	$26_{ph, pa}$	$31_{ph, pa}$
Quartz	21	4	–	2	25	27	37
Chlorite	tr	2	tr	6	17	11	2
Actinolite	–	3	–	–	–	–	–
Albite	–	–	–	1	–	–	–
Calcite	–	–	–	–	–	2	–
Rutile	2	2	4	2	–	–	tr
Sphene	1	2	–	1	–	–	–
Opaque	–	tr_{py}	2_{py}	tr_{py}	–	tr_{py}	5_{ilm}
Apatite	tr	–	–	–	–	–	tr

Note: tr < 0.5; ph—phengite; pa—paragonite; py—pyrite; ilm—ilmenite.

Geothermobarometry

The temperature of peak metamorphism can be estimated from the distribution of Fe^{2+} and Mg between adjoining garnet and omphacite pairs. Although several recent calibrations of the garnet-clinopyroxene Fe-Mg geothermometer have been made, they differ insignificantly from the original experimental calibration of Ellis and Green (1979). The Fe^{2+}/Mg distribution coefficient between garnet and omphacite [$K_D = (Fe^{2+}/Mg)_{garnet}/(Fe^{2+}/Mg)_{omphacite}$] of eclogite samples 9C and 10B cluster about 35, giving a metamorphic temperature of 450 °C for a given pressure of 17 kbar. K_D values from eclogite sample 7 are consistently lower (15–20) and indicate higher temperatures of ~540 °C at 17 kbar (Fig. 9).

Mineral assemblages with chloritoid and glaucophane are common in many HP metamorphic belts, including Oman (El-Shazly and Liou, 1991), the Western Alps (Chopin, 1981), Alaska (Forbes et al., 1984; Patrick and Evans, 1989), Greece (Schliestedt, 1986; Theye and Seidel, 1991), and other regions (e.g., Faryad, 1995). At 500–525 °C chloritoid-glaucophane is replaced by paragonite and garnet by the mineral equilibria (Fig. 9):

Ferrochloritoid + ferroglaucophane + quartz = paragonite + almandine + H_2O. (1)

Magnesiochloritoid + ferroglaucophane + quartz = glaucophane + paragonite + almandine + H_2O. (2)

These equilibria were calculated for the analyzed chloritoid-glaucophane mica schists from the Domuzdağ Complex using the THERMOCALC program (v. 2.75) of Powell and Holland (1988) with the thermodynamic data set of Holland and Powell (1998). The activities used in equilibria leading to the *P-T* estimation are shown in Table 2. They were obtained using the AX program of T.J.B. Holland (www.esc.cam.ac.uk/astaff/holland). The program uses ideal site mixing for sodic amphibole, two-site non-ideal mixing for chloritoid ($W_{Fe, Mg}$ = 1.5 kJ), two-site mixing with regular solution for jadeite (Wjd, di = 24 kJ, $W_{jd, ac}$ = 0 kJ), non-ideal mixing for phengite and paragonite, and regular solution model for garnet (Wpy, alm = 2.5 kJ, Wgr, py = 33 kJ). Mineral equilibria 1 and 2 indicate metamorphic temperatures of 475 to 500 °C at 17 kbar, similar to the peak temperatures estimated in other chloritoid-glaucophane–bearing terranes (e.g., Schliestedt, 1986; El-Shazly and Liou, 1991; Patrick and Evans, 1989).

The presence of paragonite and jadeitic clinopyroxene in the HP-LT metamorphic rocks of

TABLE 2. REPRESENTATIVE MINERAL COMPOSITIONS FROM THE HP-LT METAMORPHIC ROCKS OF THE DOMUZDAĞ COMPLEX

	Eclogite 9C					Eclogite 10B							Chloritoid-glaucophane schist 758B					
	gt rim	cpx	laws inc	glau	epidote	ph	gt core	gt rim	cpx	laws lnc	epidote	ph	pa	gt core	gt rim	ctd	glau	ph	pa	chl
SiO_2	37.86	56.01	38.69	58.71	38.51	50.83	37.29	37.72	56.29	38.79	38.43	49.14	47.23	36.02	36.58	24.02	57.56	50.55	46.29	24.15
TiO_2	0.06	0.08	0.14	0.02	0.19	0.23	0.04	0.08	0.02	0.12	0.04	0.24	0.00	0.06	0.06	0.05	0.04	0.18	0.06	0.08
Al_2O_3	21.11	9.08	31.11	11.16	26.46	25.70	20.59	20.95	9.42	30.98	26.12	25.81	38.20	20.85	21.11	40.47	11.90	25.38	39.34	20.25
Cr_2O_3	nd	nd	nd	nd	nd	nd	nd	nd	nd	Nd	nd	nd	nd	0.00	0.03	0.06	0.02	0.09	0.00	0.06
FeO	30.41	5.62	0.74	8.51	8.30	2.31	32.88	30.70	5.02	2.47	8.71	2.33	0.70	30.81	33.28	24.14	11.94	3.12	0.37	32.84
MgO	2.92	8.65	0.00	11.42	0.05	3.79	1.66	3.01	8.43	0.08	0.00	3.16	0.31	1.16	1.57	2.80	8.09	3.26	0.15	10.07
MnO	0.46	0.00	0.02	0.09	0.05	0.06	0.98	0.33	0.00	0.09	0.14	0.05	0.06	6.79	2.26	0.21	0.06	0.00	0.00	0.25
CaO	8.47	14.14	17.75	0.80	23.93	0.00	7.62	8.23	13.78	16.99	23.53	0.01	0.09	4.16	5.54	0.01	0.09	0.00	0.03	0.01
Na_2O	0.04	6.62	0.05	7.00	0.00	0.32	0.00	0.00	6.58	0.01	0.03	0.55	6.85	0.03	0.05	0.00	7.21	0.19	7.42	0.02
K_2O	0.01	0.00	0.03	0.02	0.00	10.69	0.06	0.03	0.00	0.01	0.00	10.29	0.76	0.00	0.00	0.01	0.03	10.39	0.58	0.00
Total	101.34	100.20	88.53	97.73	97.49	93.93	101.12	101.05	99.54	89.54	97.00	91.58	94.20	99.88	100.48	91.77	96.94	93.16	94.24	87.73
	12 oxy	4 cat	8 oxy	23 oxy	8 cat	11 oxy	12 oxy	12 oxy	4 cat	8 oxy	8 cat	11 oxy	11 oxy	12oxy	12oxy	12 oxy	23 oxy	11 oxy	11 oxy	14 oxy
Si	2.98	1.99	2.03	7.97	3.00	3.45	2.98	2.98	2.01	2.03	3.02	3.42	3.05	2.95	2.95	2.00	8.00	3.46	2.99	2.66
Al^4	0.02	0.01	0.00	0.03	0.00	0.55	0.02	0.02			0.00	0.58	0.95	0.05	0.05	0.00	0.00	0.54	1.01	1.34
Al^6	1.94	0.37	1.93	1.76	2.44	1.50	1.92	1.93	0.40	1.91	2.42	1.54	1.96	1.96	1.96	3.97	1.95	1.51	1.98	1.29
Ti	0.00	0.00	0.00	0.00	0.01	0.01	0.00	0.01	0.00	0.00	0.00	0.01	0.00	0.01	0.01	0.00	0.00	0.01	0.00	0.01
Cr														0.00	0.00	0.00	0.00	0.01	0.00	0.01
Fe^{3+}	0.06	0.09	0.03	0.12	0.54		0.08	0.06	0.06	0.09	0.57			0.03	0.03	0.03	0.00			
Fe^{2+}	1.95	0.08		0.84		0.13	2.12	1.97	0.09	0.02		0.14	0.04	2.08	2.22	1.66	1.39	0.18	0.02	3.03
Mg	0.34	0.46	0.00	2.31	0.01	0.38	0.20	0.35	0.45	0.01	0.00	0.33	0.03	0.14	0.19	0.35	1.68	0.33	0.01	1.66
Mn	0.03	0.00	0.00	0.01	0.00	0.00	0.07	0.02	0.00	0.00	0.01	0.00	0.00	0.47	0.15	0.02	0.01	0.00	0.00	0.02
Ca	0.71	0.54	1.00	0.12	2.00	0.00	0.65	0.70	0.53	0.95	1.98	0.00	0.01	0.36	0.48	0.00	0.01	0.00	0.00	0.00
Na	0.01	0.46	0.01	1.84	0.00	0.04	0.00	0.00	0.46	0.00	0.00	0.07	0.86	0.00	0.00	0.00	1.94	0.03	0.93	0.00
K	0.00	0.00	0.00	0.00	0.00	0.93	0.01	0.00	0.00	0.00	0.00	0.91	0.06	0.00	0.00	0.00	0.01	0.91	0.05	0.00
Total	8.04	4.00	5.00	15.00	8.00	6.99	8.05	8.04	4.00	5.01	8.00	7.00	6.96	8.05	8.04	8.04	14.99	6.98	6.99	10.02
activities at 17 kbar and 500 °C:																				
pyr	0.0054	di 0.46		gl 0.26	cz 0.55	mu 0.37	pyr 0.001	0.0056	di 0.45		cz 0.43	mu 0.41		pyr	0.00077	fct 0.81	gl 0.21	mu 0.36	daph	0.085
alm	0.22	hd 0.083		fgl 0.032		cel 0.18	alm 0.30	0.22	hd 0.12			cel 0.15		alm	0.33	mct 0.20	fgl 0.137	cel 0.16	cln	0.048
gr	0.016	jd 0.38					gr 0.0095	0.015	jd 0.40										ames	0.0093

Note: The Fe^{3+} in the sodic amphibole was calculated assuming 23 oxygens and 15 cations in the formula unit. In the sodic pyroxene the ferric iron was taken as Fe^{3+} = Na-Al. Abbreviations: inc—inclusions; nd—not determined; alm—almandine; ames—amesite; cel—celadonite; chl—chlorite; clin—clinochlore; cpx—omphacite; ctd—chloritoid; cz—clinozoisite; daph—daphnite; di—diopside; fct—ferrochloritoid; fgl—ferroglaucophane; gl—glaucophane; glau—sodic amphibole; gr—grossular; gt—garnet; hd—hedenbergite; jd—jadeite; laws—lawsonite; mct—magnesiochloritoid; mu—muscovite; pa—paragonite; ph—phengite; pyr—pyrope.

the Domuzdağ Complex constrains the metamorphic pressure between 14 and 26 kbar on the basis of the reactions (Fig. 9):

Paragonite = jadeite + kyanite + quartz. (3)

Albite = jadeite + quartz. (4)

Metamorphic pressures can further be constrained by equilibria involving garnet, clinopyroxene, and phengite (Fig. 9):

Diopside + muscovite =
pyrope + grossular + celadonite. (5)

Diopside + hedenbergite + muscovite =
almandine + grossular + celadonite. (6)

These reactions indicate metamorphic pressures of 17–20 kbar at 500 °C. Average pressure calculations with THERMOCALC, using all the matrix phases in the eclogites, give 17.1 ± 1.3 kbar and 15.6 ± 3.5 kbar at 500 °C for eclogite samples 10B and 9C, respectively. The estimated peak *P-T* conditions in the Domuzdağ Complex are, therefore, 490 ± 20 °C and 17 ± 2 kbar. The temperature estimate is based largely on the garnet-glaucophane-chloritoid equlibria in mica schists, and the pressure estimate on the garnet-omphacite-phengite equilibria in the eclogites (Fig. 9). These *P-T* conditions plot on the boundary between epidote-blueschist and the eclogite facies of Evans (1990).

Lawsonite must have been formerly present in the Domuzdağ metabasites, as shown by the common lawsonite inclusions in garnets (Altherr et al., 2004). Lawsonite must have reacted with the sodic pyroxene to produce garnet and epidote on the basis of the reactions (Fig. 9):

Lawsonite + jadeite =
grossular + paragonite + quartz + H_2O. (7)

Lawsonite + jadeite =
clinozoisite + paragonite + quartz + H_2O. (8)

These reactions, calculated from the mineral compositions of eclogite sample 10B, pass through the broad *P-T* field determined from the matrix phases (Fig. 9), suggesting that the upper temperature stability field of lawsonite has just been exceeded. In Fe^{3+}-poor rocks the stability of lawsonite will extend toward higher temperatures, which would explain its presence as a matrix phase in some metasedimentary rocks.

The accretionary complex character of the Domuzdağ Complex implies that it must consist of a large number of individual tectonic slices; the boundaries of individual slices, however, are

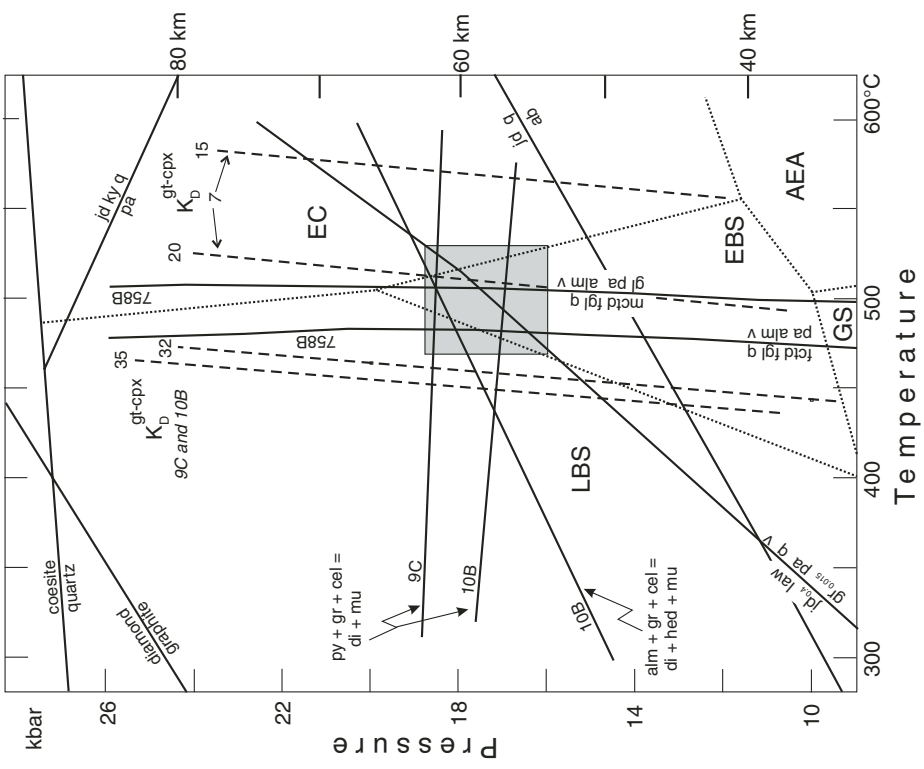

Figure 9. Pressure-temperature (*P-T*) diagram, showing equilibria relevant to the estimation of *P-T* conditions of the Domuzdağ Complex. Facies boundaries are after Evans (1990). LBS—lawsonite blueschist; EBS—epidote blueschist; EC—eclogite; AEA—albite-epidote amphibolite; GS—greenschist facies. All reactions were calculated using THERMOCALC program of Powell and Holland (1988) and Holland and Powell (1998). Other abbreviations: K_D—K_D-$(Fe^{2+}/Mg)_{garnet}/(Fe^{2+}/Mg)_{omphacite}$; ab—albite; alm—almandine; cel—celadonite; cpx—clinopyroxene; di—diopside; fctd—ferrochloritoid; fgl—ferroglaucophane; gl—glaucophane; gt—garnet; hed—hedenbergite; jd—jadeite; ky—kyanite; law—lawsonite; mctd—magnesiochloritoid; mu—muscovite; pa—paragonite; py—pyrope; q—quartz; v—H_2O.

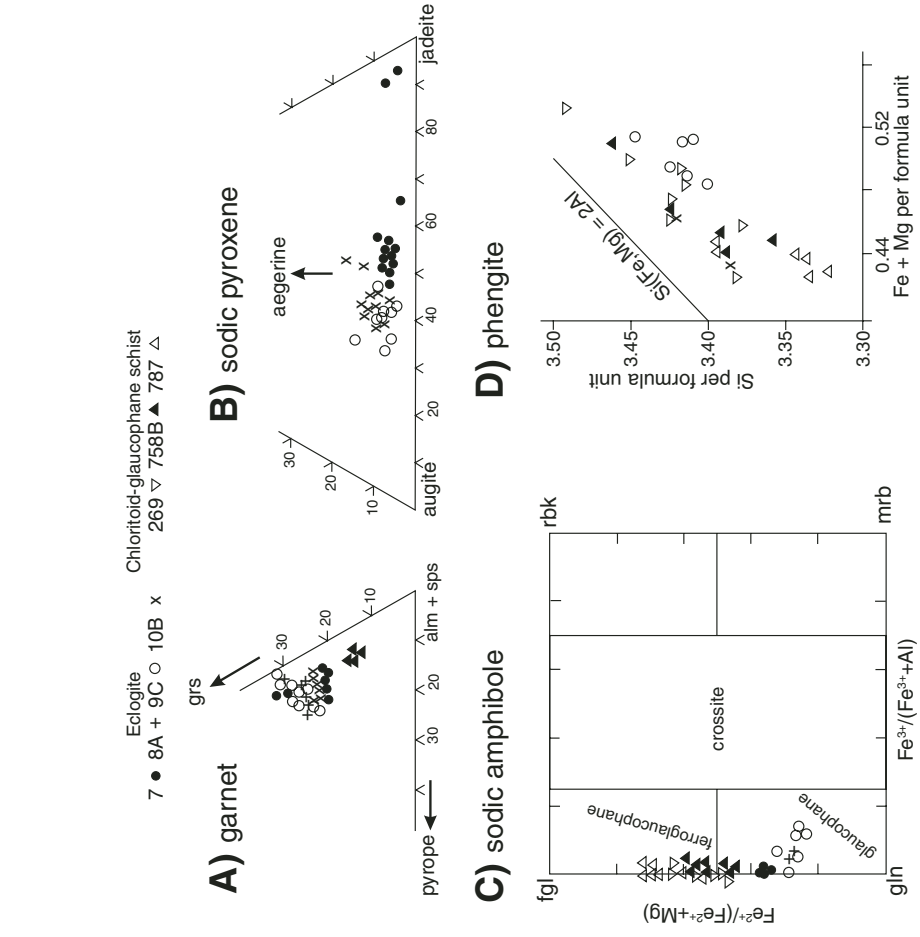

Figure 8. Garnet, sodic pyroxene, sodic amphibole, and phengite compositions from the eclogites and chloritoid-glaucophane mica schists of the Domuzdağ Complex. Abbreviations: alm—almandine; fgl—ferroglaucophane; gln—glaucophane; mrb—magnesioriebeckite; rbk—riebeckite; sps—spessartine; grs—grossular.

difficult to map except in the case of ophiolite fragments. The individual tectonic slices must have been metamorphosed at slightly different times and at different depths in the oceanic subduction zone. The higher metamorphic temperatures from eclogite sample 7 (Fig. 9) might be an indication of the independent *P-T-t* [time] history of an individual tectonic slice within the Domuzdağ Complex. The estimated *P-T* conditions for the Domuzdağ Complex must therefore be viewed as a broad pressure-temperature window under which underplating took place rather than that of a coherent regional metamorphic terrane.

TABLE 3. Ar-Ar ISOTOPIC DATA ON PHENGITE FROM THE ECLOGITE 9C SAMPLE

	$^{36}Ar/^{39}Ar$	±	$^{37}Ar/^{39}Ar$	±	$^{38}Ar/^{39}Ar$	±	$^{40}Ar/^{39}Ar$	±	$^{40}Ar^*/^{39}Ar$	±	Age (Ma)	± (1σ)
1	0.0091	0.0001	62.273	0.0143	0.0211	0.0003	111.298	0.0191	84.543	0.0386	95.1	0.6
2	0.0678	0.0011	339.832	0.2143	0.0647	0.0008	286.600	0.1636	86.179	0.3201	96.9	3.5
3	0.0138	0.0003	104.552	0.0723	0.0231	0.0002	128.185	0.0156	87.277	0.0826	98.1	1.0
4	0.0030	0.0001	0.9073	0.0047	0.0141	0.0001	96.499	0.0180	87.556	0.0250	98.4	0.5
5	0.0037	0.0003	31.381	0.0477	0.0128	0.0007	98.791	0.0932	87.909	0.1364	98.7	1.6
6	0.0874	0.0045	878.141	0.7061	0.1163	0.0038	347.338	0.1327	89.117	13.408	100.1	14.7
7	0.0163	0.0004	281.699	0.1510	0.0492	0.0018	138.038	0.0865	89.933	0.1386	101.0	1.6
8	0.1158	0.0022	294.503	0.1687	0.1547	0.0015	438.141	0.1890	95.906	0.6486	107.5	7.1
9	0.0897	0.0013	348.287	0.2349	0.1248	0.0018	361.463	0.1769	96.310	0.3580	107.9	3.9
10	0.6114	0.0067	655.916	0.6925	0.4259	0.0065	1,906.066	17.609	99.443	10.861	111.3	11.8
11	0.0533	0.0032	274.185	0.2642	0.0727	0.0032	259.130	0.0964	101.697	0.9349	113.8	10.1
12	0.1055	0.0021	465.478	0.5673	0.1383	0.0031	413.529	0.2819	101.836	0.6126	113.9	6.7
13	0.0403	0.0010	631.963	0.4616	0.0942	0.0015	223.241	0.1266	104.210	0.3092	116.5	3.4

Isotopic Age Data

Ar-Ar and Rb-Sr isotopic analyses were carried out on four eclogites and one mica schist from the Domuzdağ Complex to date the HP-LT metamorphism. The analytical conditions are described in the Appendix. The isotopic age data are given in Tables 3 and 4, and the locations of the dated samples are shown in Figure 3. The only previous age data from the Domuzdağ Complex were six K-Ar whole-rock, phengite, and glaucophane ages published by Ustaömer and Robertson (1997). Their whole-rock K-Ar ages showed a scatter from 37 to 106 Ma, whereas the phengite and glaucophane K-Ar ages were 83.7 ± 9.7 Ma and 106.8 ± 4.7 Ma, respectively. These ages were interpreted as the thermal resetting of the late Paleozoic–Triassic HP-LT metamorphism.

TABLE 4. Rb-Sr ISOTOPIC DATA FROM THE CENTRAL PONTIDES

Sample	Mineral	Rb (ppm)	Sr (ppm)	$^{87}Rb/^{86}Sr$	$^{87}Sr/^{86}Sr$	Age (Ma)
Chloritoid–mica schist						
247	Rock	153.4	98.30	4.5212	0.723913 ± 10	
	Phengite	12.11	858.30	0.0408	0.717271 ± 10	104.3 ± 4.8
	Chloritoid	0.559	1370	1.1811	0.717387 ± 20	137.5 ± 6.6
Eclogite						
440	Rock	14.0	142.0	0.2852	0.707620	
	Phengite	131.5	14.9	25.64	0.746055	107 ± 1
441	Rock	18.0	504.0	0.1033	0.707287	
	Phengite	94.0	116.1	2.343	0.711230	124 ± 9
444	Rock	13.0	50.0	0.7521	0.705640	
	Phengite	49.8	16.3	8.860	0.717820	106 ± 3

The eclogite dated by the Ar-Ar method (sample 9C) consists roughly of equal amounts of garnet, omphacite, and glaucophane, which together make up 90% of the rock (Table 1). Phengite grains, 0.2–0.4 mm long, occur in amounts of ~2 modal%. Fourteen individual Ar-Ar spot ages range from 95.1 ± 0.6 to 116.5 ± 3.4 Ma (Table 3) with a mean age of 104.5 ± 7.2 Ma. On an inverse isochron correlation diagram, the data form a trend that intercepts at a $^{40}Ar/^{36}Ar$ value of 305 ± 13 and yields an intercept age of 99.5 ± 1.3 Ma. The proximity of the $^{40}Ar/^{36}Ar$ ratio to air (295.5) suggests that any contamination from excess argon is minimal and probably close to detection limits. Most of the "older" ages have much larger uncertainties and slightly elevated $^{37}Ar_{Ca}/^{39}Ar_K$ ratios, which indicate there may be some contamination by a calcic phase within the laser spot analyses.

The Rb-Sr phengite ages from the three eclogites are 106 ± 3 Ma, 107 ± 1 Ma, and 124 ± 9 Ma (Table 4). The dated chloritoid mica schist (sample 247) consists of phengite (57% of the mode), quartz (28%), chloritoid (12%), and opaque (3%). Most of the rock consists of phengite, which forms grains 0.5 mm long, associated with smaller chloritoid grains 0.1–0.3 mm long. The Rb-Sr phengite age from this sample is 104 ± 5 Ma, comparable to the other Rb-Sr and Ar-Ar phengite ages.

The closure temperature for the Ar/Ar system for the coarse phengite grains is probably 400 ± 50 °C (e.g., Purdy and Jäger, 1976; Sherlock et al., 1999) and in the Rb-Sr system 500 ± 50 °C (Jäger et al., 1967). The ~490 °C maximum temperature during the regional metamorphism, and the inferred rapid exhumation of the HP-LT metamorphic rocks (see later discussion), indicate that the phengite ages correspond to the age of the peak metamorphism. The Ar-Ar and Rb-Sr phengite ages from the Domuzdağ Complex are coherent and indicate that the HP-LT metamorphism of the Domuzdağ Complex is Cretaceous in age and took place during the Albian at 105 ± 5 Ma.

The subduction, accretion, and underplating in a subduction zone occur over a time span, which in places is reflected in the geochronology. For example, geochronological data from the Franciscan Complex indicate that subduction and HP-LT metamorphism took at least 75 m.y. (cf. Wakabayashi, 1999). The limited geochronological data from the Domuzdağ Complex, on the other hand, imply a short time span for the HP-LT metamorphism. This and the general absence of arc magmatism in the Pontides during the Late Jurassic–Early Cretaceous suggest only a short period of subduction before the underplating of the Domuzdağ Complex.

Interpretation of the Domuzdağ Complex

The HP-LT regional metamorphism, the presence of ophiolite fragments and deep marine sediments such as metacherts, and the MORB-type geochemistry of the metabasites indicate that the Domuzdağ Complex represents a subduction complex (Tüysüz, 1990; Tüysüz and Yiğitbaş, 1994; Ustaömer and Robertson, 1997, 1999). The mica schists in the Domuzdağ Complex were probably trench sediments, and the metabasite, metagabbro, metachert, and serpentinite are underplated fragments of the Tethyan oceanic lithosphere. Ustaömer and Robertson (1997, 1999) interpreted the Domuzdağ Complex as a subduction-accretion unit produced during the northward subduction of the Paleo-Tethys. We concur with their model except for the age of subduction, which is Early Cretaceous rather than Triassic.

TECTONIC UNITS ABOVE THE HP-LT METAMORPHIC ROCKS

Çangaldağ Complex

This is a pre-Jurassic metabasite-phyllite-marble unit, which forms two crustal-scale tectonic slices north and south of the Gökırmak fold-and-thrust belt (Fig. 2). In its northern outcrop the Çangaldağ Complex is intruded by mid-Jurassic granitic rocks that provide a constraint on its age (Yılmaz, 1980; Yılmaz and Boztuğ, 1986; Aydın et al., 1995).

In its southern outcrop the Çangaldağ Complex forms a northward-dipping tectonic slice, ~5 km in structural thickness (Figs. 2 and 3), lying directly on the Domuzdağ Complex. The basal contact of the Çangaldağ Complex with the Domuzdağ Complex is a 50°–60° north-dipping shear zone. The HP-LT metamorphic rocks of the Domuzdağ Complex exhibit gradual retrogression into greenschist facies rocks toward this Acısu Fault, over a transition zone of several hundred meters. In the shear zone the eclogites are completely transformed into banded, mylonitized, medium grained albite-chlorite gneisses. Mylonitization is largely confined to the footwall of the Acısu Fault. Microscopic and mesoscopic microstructural criteria for the sense of shear in the mylonite zone are ambiguous. The Acısu Fault emplaces lower-grade and older Çangaldağ Complex rocks over the higher-grade and younger Domuzdağ Complex. It is therefore regarded as a Late Cretaceous shear zone with a normal sense of movement, which facilitated the exhumation of the Domuzdağ Complex. Nevertheless, imbrication of the Çangaldağ and Domuzdağ tectonic slices north of Kovaçayır (Fig. 3) suggests that at least parts of the Acısu Fault were reactivated as a thrust in the Cretaceous or later.

The lower 1 km of the Çangaldağ sequence is dominated by phyllite and chlorite-albite mica schist with rare marble and metabasite layers, which are a few meters to several tens of meters thick. The upper 4 km is made up mainly of metabasite (>70% of the outcrops) with phyllite and marble layers. Marble makes up <3% of the Çangaldağ sequence. The protoliths of the metabasic rocks are mainly tuffs and fine-grained pyroclastic rocks, and rarely lava flows and diabase. There are also small (<100 m) metagabbro lenses within the metabasites. A penetrative foliation, with an average strike of N67°E and a dip of 40° to the north, is prominent in the phyllites, albite-chlorite schists, and fine-grained metabasites (Fig. 5). An indistinct subhorizontal mineral lineation in the metabasic rocks trends ENE.

The Çangaldağ Complex has undergone a low-grade regional metamorphism in high-pressure greenschist facies. In the coarse-grained metabasites, magmatic augite is commonly preserved. The common mineral assemblage in the metabasic rocks is actinolite-barroisite + epidote + albite + chlorite + sphene ± pumpellyite ± sodic amphibole ± relict augite (Fig. 6). Sodic amphibole occurs as rims around actinolite or as incipient grains growing around relict augite. The phyllites in the Çangaldağ Complex are characterized by quartz + white mica + chlorite paragenesis.

In the north the Çangaldağ Complex is unconformably overlain by Maastrichtian or Eocene sedimentary rocks. Northeast of the village of Akçasu, thickly bedded neritic limestones of Maastrichtian age—with the large benthic foraminifers *Siderolites* sp., *S. calcitrapoides* Lamarck, *Sirtina* sp., *Hellenocyclina beotica* Reichel, and *Orbitoides* sp.—lie unconformably over the metabasites through a basal conglomerate consisting of clasts of the underlying metamorphic rocks (Fig. 3). West of Akçasu, the metamorphic rocks are unconformably overlain by limestones and pelagic marls of late Paleocene (Thanetian) age with *Acarinina* sp., *A. mckannai* (White), *Morozovella* sp., *M. aequa* (Cushman and Renz), and transported *Nummulites* sp. (Toumarkine and Lutherbacher, 1985).

In its second large outcrop north of the Gökırmak fold-and-thrust belt, the Çangaldağ Complex makes up a northward-dipping, structurally thickened 10-km-thick sequence dominated by metabasic rocks (Fig. 2; Yılmaz, 1980, 1983; Ustaömer and Robertson, 1997, 1999). Intercalated with the metabasites are minor phyllite, metaandesite, metadacite, metarhyolite, and marble. The protoliths of the metabasites are mainly pyroclastic and epiclastic rocks with minor lava flows and dikes. As with the southern outcrop of the Çangaldağ Complex, small metagabbro, metadiabase, and more metafelsic intrusives occur, which are <100 m across. The regional metamorphism is in greenschist facies, and no sodic amphibole is reported from the northern Çangaldağ Complex (Yılmaz, 1983). Ustaömer and Robertson (1999) studied in detail the geochemistry of the northern Çangaldağ Complex. In the trace element diagrams the compositions of the metavolcanic rocks plot in the fields of basaltic andesite, andesite, and rhyodacite; and in the tectonic discrimination diagrams the metavolcanic rocks plot mostly in the field of island arc tholeiite. Ustaömer and Robertson (1997, 1999) interpret the Çangaldağ Complex as a Late Permian–Early Triassic, south-facing, intra-oceanic magmatic arc, accreted to the southern margin of Eurasia during the latest Triassic–Early Jurassic Cimmerian orogeny. In terms of lithology, tectonostratigraphy, metamorphism, and structure, the Çangaldağ Complex is similar to the Nilüfer Formation of northwest Turkey, which is interpreted as an accreted Paleo-Tethyan oceanic plateau or a series of oceanic islands (Okay, 2000; Okay and Göncüoğlu, 2004; Pickett and Robertson, 2004). The regional metamorphism in the Nilüfer Formation is isotopically dated as latest Triassic, using the Ar-Ar method on phengite (Okay et al., 2002), and the marble layers in the Nilüfer Formation have yielded conodonts of Early and Middle Triassic ages (Kaya and Mostler, 1992; Kozur et al., 2000).

Gökırmak Fold-and-Thrust Belt

A fold-and-thrust belt made up of Cretaceous to Eocene sedimentary and volcanic rocks is sandwiched between the southern and northern Çangaldağ Complexes (Fig. 2). The fold-and-thrust belt represents the southernmost outcrops of the Cretaceous–Eocene series of the Black Sea margin (Fig. 2; Gedik and Korkmaz, 1984; Görür and Tüysüz, 1997). The structure in the fold-and-thrust belt is characterized by south-vergent thrusts and recumbent folds, ranging from outcrop to kilometer scale (Fig. 4). The belt forms part of the major south vergent Ekinveren thrust zone (Fig. 2). Eocene rocks are involved in folding and thrusting; major angular unconformities in the sequence, however, suggest that deformation also occurred episodically during the Late Cretaceous and Paleocene. The stratigraphy and depositional environment in the fold-and-thrust belt are important for establishing the tectonic setting before, during, and after the emplacement of the HP-LT metamorphic rocks. With this aim, we mapped the Gökırmak fold-and-thrust belt in detail and measured several stratigraphic sections (Figs. 10 and 11).

Çağlayan Formation

The lowest exposed unit in the fold-and-thrust belt is a highly deformed olistostromal turbidite sequence, >2000 m thick, consisting of dark shales interbedded with thin to medium bedded sandstones that comprise grain flows, debris flows, and olistostromes with clasts of metabasite, phyllite, and Jurassic limestone up to several kilometers across (Fig. 11). No age-diagnostic fossils have been found in the Çağlayan Formation. Generally an Early Cretaceous (Barremian to Albian) age is accepted for the Çağlayan Formation on the basis of scarce foraminifers and nannoplankton (Gedik and Korkmaz, 1984; Aydın et al., 1986, 1995).

The Çağlayan Formation crops out over large areas in the Central Pontides, and in the

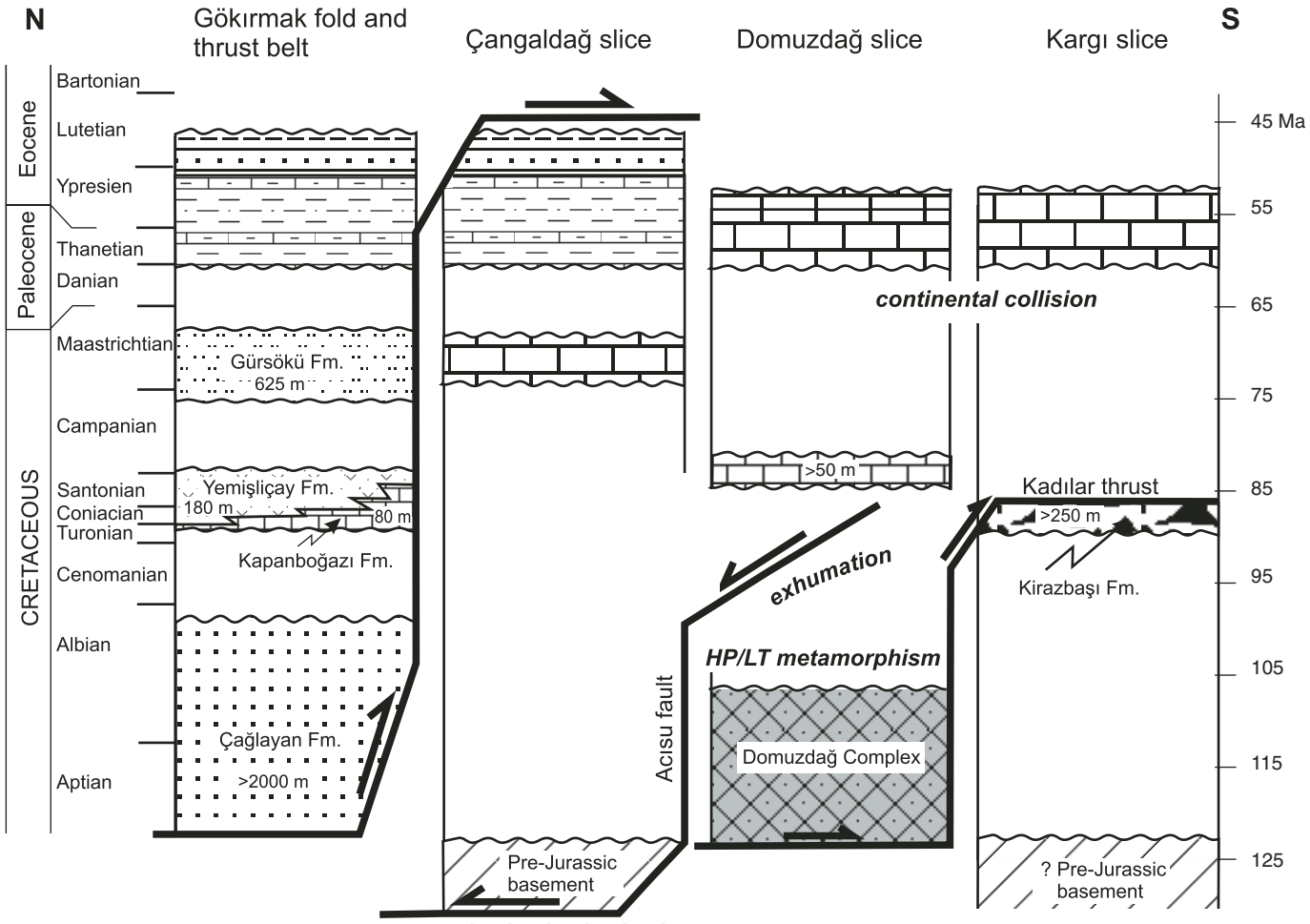

Figure 10. Generalized stratigraphic sections of the Gökırmak fold-and-thrust belt and the Çangaldağ, Domuzdağ, and Kargı tectonic slices.

few localities where its base is observed, it rests unconformably over the Upper Jurassic–Lower Cretaceous neritic carbonates. It is generally interpreted as an Early Cretaceous syn-rift sequence related to the opening of the Black Sea basin (Görür, 1988; Robinson et al., 1995, 1996; Tüysüz, 1999). Its deposition overlaps the HP-LT metamorphism in the Central Pontides. The Çağlayan Formation does not extend into the Eastern Pontides, where the Barremian–Albian interval is characterized by nondeposition or erosion (e.g., Pelin, 1977; Robinson et al., 1995; Okay and Şahintürk, 1997; Rojay, 1995).

Kapanboğazı Formation

The Çağlayan Formation is unconformably overlain by the red pelagic limestones of the Kapanboğazı Formation, rich in foraminifers and radiolarians and with a thickness ranging from a few meters up to 160 m (Fig. 10). The Kapanboğazı Formation consists dominantly of thinly bedded red pelagic micrites with thin shaly partings and beds. There are also rare grain and debris flows, made up of metamorphic rock fragments. Several sections were measured in the Kapanboğazı Formation to constrain its biostratigraphy (Fig. 11). In the 26-m-thick Vakıf section, a sample 3 m above the base of the Kapanboğazı Formation gives a Santonian age on the basis of the planktonic foraminiferal assemblage: *Marginotruncana coronata* (Bolli), *M. pseudolinneiana* Pessagno, *M. sigali* (Reichel), *M. sinuosa* Porthault, *Heterohelix moremani* (Cushman), *Hedbergella* spp., *Globotruncana bulloides* Vogler, *Globotruncanita elevata* (Brotzen) (Caron, 1985; Premoli Silva and Sliter, 1994; Robaszynski et al., 2000) (Fig. 12K–M). The rest of the samples give a wider Santonian–Coniacian age. A point sample from the Kapanboğazı Formation (413A) contains the planktonic foraminifer *Dicarinella asymetrica* (Sigal), the type fossil for the upper zone of the Santonian (Caron, 1985; Premoli Silva and Sliter, 1994; Robaszynski, et al., 2000). Therefore, the age of the Kapanboğazı Formation in the area studied is Santonian, possibly extending down to Coniacian.

The Kapanboğazı Formation forms a marker zone throughout the Central and Eastern Pontides (Pelin et al., 1982; Görür et al., 1993) and is interpreted as a postrift sequence deposited following the formation of the first oceanic crust in the Black Sea backarc basin (Görür, 1988; Görür et al., 1993). Paleomagnetic analyses of the Kapanboğazı Formation in the area studied indicate a paleolatitude of 21.5°N, placing it between West Gondwana and Eurasia (Channell et al., 1996) with the implication that the West Black Sea oceanic basin was open by the Coniacian–Santonian.

Yemişliçay Formation

The Kapanboğazı Formation passes laterally and upward to a sequence of volcanic agglomerate, tuff, and pelagic limestone 125–250 m in thickness. Pelagic limestones occur both as interbeds and as blocks in the volcanic rocks. Pelagic limestones sampled from the basal and upper parts of the Yemişliçay Formation contain planktonic foraminifers characteristic of

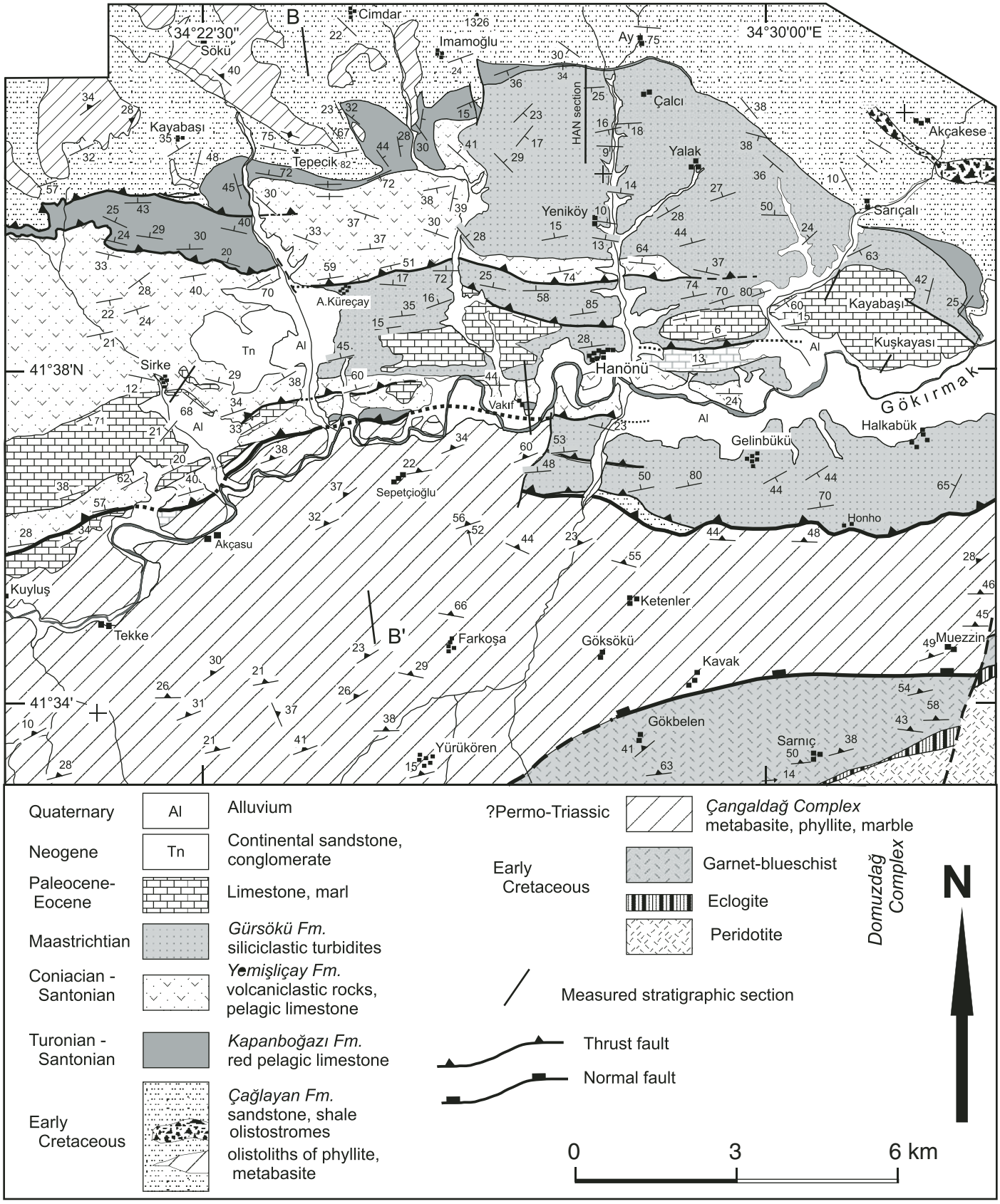

Figure 11. Geological map of the Gökırmak fold-and-thrust belt. For location, see Figure 2, and for the cross section, see Figure 4.

the Coniacian–Santonian: *Dicarinella primitiva* (Dalbiez), *Marginotruncana coronata* (Bolli), *M. pseudolinneiana* Pessagno, *Hedbergella* spp., and *Hetereohelix* spp. (Caron, 1985; Premoli Silva and Sliter, 1994; Robaszynski, et al., 2000). The Yemişliçay Formation was formed in a submarine magmatic arc above the northward subducting Neo-Tethyan oceanic lithosphere. The subalkaline geochemistry of the Senonian magmatic rocks from the Eastern Pontides is compatible with a subduction origin (e.g., Manetti et al., 1983; Akıncı, 1984; Çamur et al., 1996; Arslan et al., 1997).

Gürsökü Formation

A siliciclastic turbidite sequence 625 m thick, the Gürsökü Formation, lies with an angular unconformity over the Çağlayan, Kapanboğazı, and Yemişliçay Formations (Figs. 10 and 11). The Gürsökü consists of interbedded sandstone, pebbly sandstone, shale, and conglomerate. The conglomerates are polymictic, and the poorly sorted clasts include metamorphic, magmatic, and sedimentary rocks. Large benthic foraminifers of the *Orbitoides* and *Lepiorbitoides* type are relatively abundant in the coarse-grained turbiditic sandstones. On the basis of a detailed measured section (the Han section in Fig. 11), Özcan and Özkan-Altıner (1999) and Özkan-Altıner and Özcan (1999) assign a Maastrichtian and a possible late Campanian age range to the Gürsökü Formation, as determined from the benthic foraminifers. Several of our point

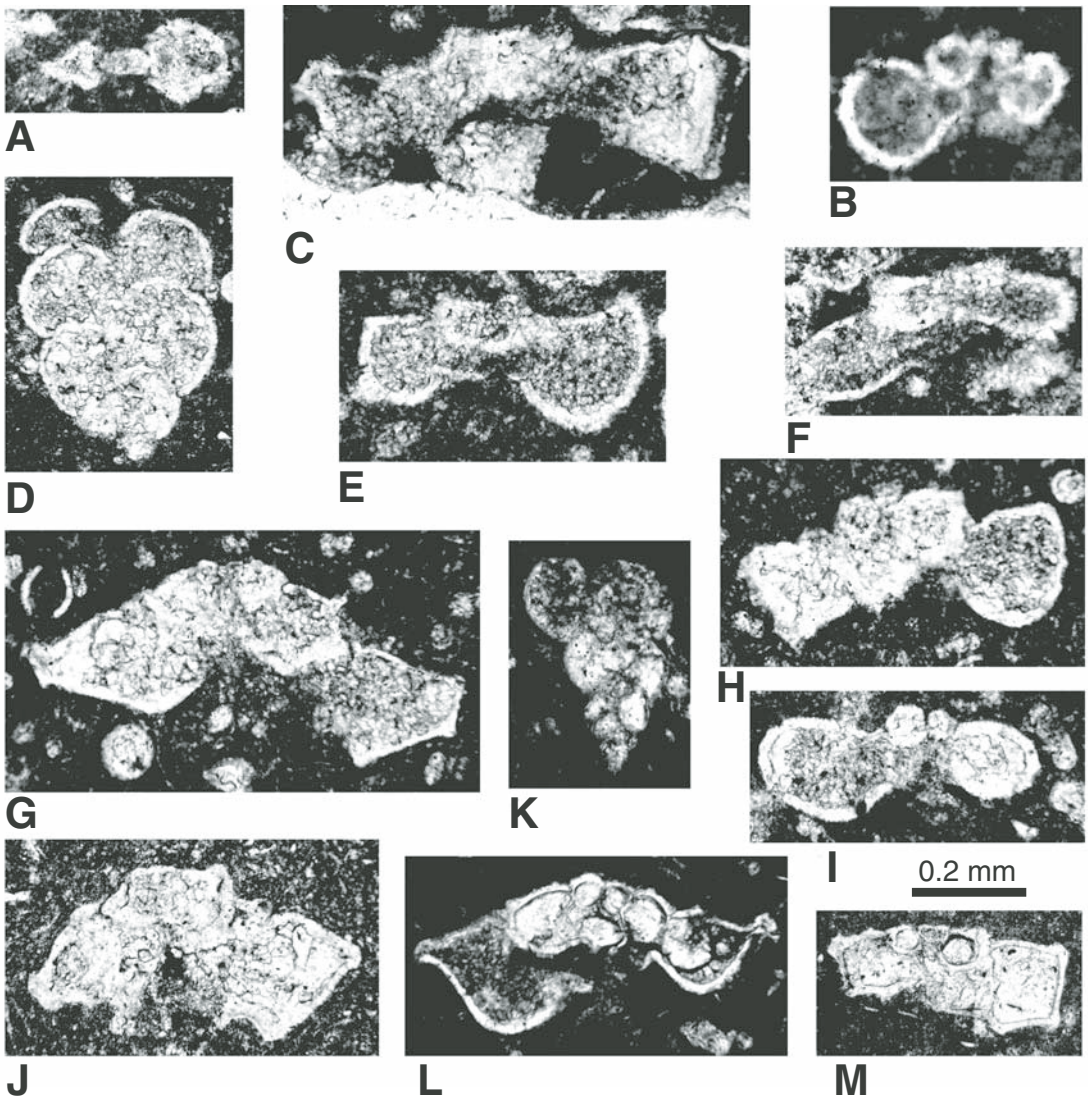

Figure 12. Photomicrographs of some important microfossils. Stratigraphic ranges are from Premoli Silva and Sliter (1994). Kirazbaşı Formation: (A) *Planomalina* cf. *buxtorfi* (Gandolfi), A-7, late Albian; (B) *Ticinella roberti* (Gandolfi), A-7, late Albian; (C) *Dicarinella asymetrica* (Sigal), A-6, Santonian; (D) *Heterohelix punctulata* (Cushman), A-6, Santonian–Maastrichtian; (E) *Helvetoglobotruncana helvetica* (Bolli), A-5, early Turonian; (F) *Dicarinella canaliculata* (Reuss), A-5, Cenomanian–Coniacian; (G) *Marginotruncana renzi* (Gandolfi), A-2, Turonian–Santonian; (H) *Globotruncana* cf. *hilli* Pesssagno, A-2, Turonian–Maastrichtian; (I) *Hedbergella flandrini* Porthault, A-2, late Turonian–Santonian; (J) *Marginotruncana sigali* (Reichel), A-3, Turonian–Santonian. Kapanboğazı Formation: (K) *Heterohelix moremani* (Cushman), V-3, Cenomanian–Campanian; (L) *Globotruncanita* cf. *elevata* (Brotzen), V-3, Santonian–Campanian; (M) *Marginotruncana pseudolinneiana* Pessagno, V-3, Santonian–Campanian.

samples include benthic foraminifers characteristic of the Maastrichtian: *Siderolites* cf. *calcitrapoides* Lamarck, *Cideina* cf. *soezerii* (Sirel), and *Lepiorbitoides* sp.

The base of the Gürsökü Formation cuts down from the Yemişliçay Formation in the south to the Çağlayan Formation in the northeast over a distance of 4 km (Fig. 11), indicating differential vertical movements, possibly related to contractional deformation in the arc massif before the deposition of the Gürsökü Formation. In the Eastern Pontides and Lesser Caucasus, an ophiolitic accretionary complex was thrust northward over the continental margin during the late Santonian–Campanian (Okay and Şahintürk, 1997). In the southern parts of the Central Pontides, turbidites of the Gürsökü Formation rest unconformably over the ophiolitic accretionary complex (Dirik, 1993; Rojay and Altıner, 1998). The widespread mid-Campanian–Maastrichtian siliciclastic turbidites in the Central and Eastern Pontides are generally interpreted as forearc flysch sequences deposited after the Santonian–Campanian deformation (Görür et al., 1984; Koçyiğit, 1991; Dirik, 1993; Rojay, 1995).

Paleocene–Eocene Carbonates

A sequence of white and pale gray limestone and marl lies unconformably over the Gürsökü and Yemişliçay Formations; they are preserved in the cores of faulted synclines along the Gökırmak valley (Fig. 11). Their age, on the basis of benthic and pelagic foraminifers and nannoplankton, is late Paleocene–early Eocene. This sequence marks a lull in the orogenic activity between the early Paleocene and mid-Eocene.

Lower Cretaceous Slate Sequence

In the west the Domuzdağ Complex is tectonically overlain by a slate sequence (Fig. 2). The contact is marked by tectonic slices of ophiolitic mélange, and is covered by Eocene and younger sedimentary rocks. The metaclastic sequence consists dominantly of yellowish brown slates, which make up 80% of the outcrops. They are intercalated with metasandstone beds 10–30 cm thick. There are also thickly bedded neritic recrystallized limestone lenses, up to several hundred meters across, from which Late Jurassic–Early Cretaceous fossils are reported (H.S. Serdar, 2000, personal commun.). The regional metamorphism is in low-grade greenschist facies. This Cretaceous slate sequence forms part of the extensive Lower Cretaceous turbidite basin in the Central Pontides (Fig. 2). The deposition and deformation of the Lower Cretaceous turbidites are associated with the collision of the Istanbul and Sakarya terranes (Tüysüz, 1999). The tectonic juxtaposition of the Domuzdağ Complex and the slate sequence must be coeval or later than the Turonian exhumation of the HP-LT metamorphic rocks.

TECTONIC UNITS BELOW THE HP-LT METAMORPHIC ROCKS

Kirazbaşı Formation—Turonian Foreland Basin Deposits

The Domuzdağ Complex is tectonically underlain by a Late Cretaceous flexural foreland basin with a metamorphic basement. Several stratigraphic sections were measured in foreland basin sequence, as its biostratigraphy constrains the timing and mode of emplacement of the HP-LT metamorphic rocks (Figs. 3 and 13A).

The Kirazbaşı Formation starts with light gray pelagic limestones, 1–8 m thick, deposited directly on the underlying metamorphic rocks (Fig. 13A, 13B). The pelagic limestones probably represent the back-bulge deposits of a foreland basin (e.g., De Celles and Giles, 1996). The thinly to medium bedded micritic limestone is rich in radiolarians and pelagic foraminifers. In the Kirazbaşı section (Fig. 3) a sample a few centimeters above the unconformity contains *Helvetoglobotruncana helvetica* (Bolli) (Fig. 12E), a foraminifer characteristic of the early Turonian (ca. 93 Ma; Gradstein et al., 2004) (Caron, 1985; Premoli Silva and Sliter, 1994; Robaszynski et al., 2000). In other sections the planktonic foraminiferal assemblage is indicative of Coniacian–Santonian or Turonian–Santonian age: *Heterohelix punctulata* (Cushman), *Dicarinella canaliculata* (Reuss), *Marginotruncana sigali* (Reichel), *M. renzi* (Gandolfi), *M. marginata* (Reuss), *M. pseudolinneiana* Pessagno,

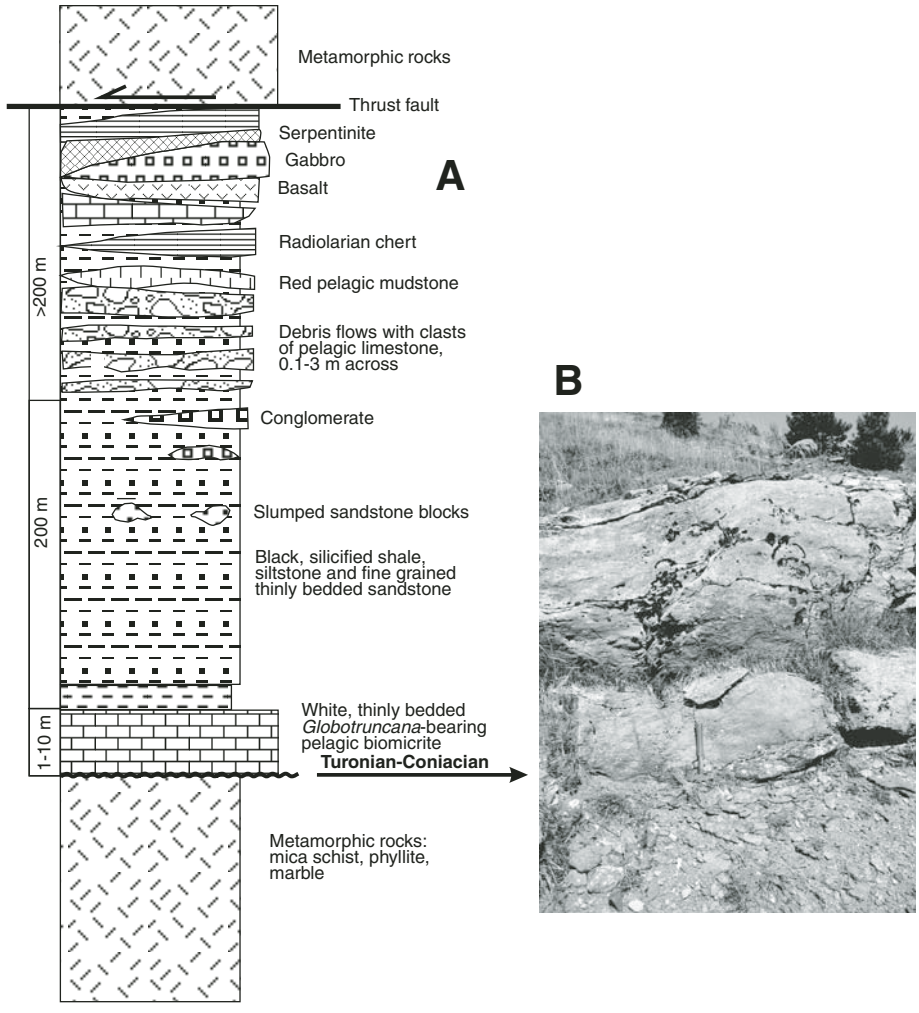

Figure 13. (A) Generalized stratigraphic section of the Kirazbaşı Formation (modified from Tüysüz, 1993). (B) Photograph showing the Turonian pelagic limestones of the Kirazbaşı Formation lying unconformably over the phyllites of the Kargı Complex. The head of the hammer lies at the contact.

M. sinuosa Porthault , *M. schneegansi* (Sigal), *M. coronata* (Bolli), *Globotruncana* cf. *hilli* Pessagno, *Hedbergella fladrini* Porthault, and *Hedbergella* spp. (Fig. 12C–I) (Caron, 1985; Premoli Silva and Sliter, 1994; Robaszynski et al., 2000). The pelagic limestones are overlain by a distal turbidite sequence of dark gray and black siliceous shale, siltstone, and thinly bedded sandstone, 200 m thick, representing the foredeep deposits (Fig. 13A). The sequence also contains thick grain and debris flow zones. The clasts in the debris flows include limestone, red mudstone, and red radiolarian chert. The 0.1–3 m large pelagic limestone blocks are of late Albian age on the basis of the planktonic foraminifers *Rotalipora ticinensis* (Gandolfi), *Rotalipora balernaensis* (Gandolfi), *Ticinella roberti* (Gandolfi), and *Planomalina* cf. *buxtorfi* (Gandolfi) (Fig. 12A, 12B). With an increase in the frequency of the debris flows, the turbidites pass up into an ophiolitic mélange of basalt, radiolarian chert, serpentinite, pelagic shale, and limestone, interpreted as the wedge-top deposits of a foreland basin. The lower parts of the ophiolitic mélange show olistostromal features, and the upper parts, tectonic features. The ophiolitic mélange makes up >90% of the outcrops of the Kirazbaşı Formation. Apart from the ophiolitic material, the mélange includes blocks and tectonic slices of metabasite, mica schist, and marble, most probably derived from the overlying Domuzdağ Complex (Tüysüz, 1985, 1990; Yiğitbaş et al., 1990).

The structural position of the Kirazbaşı Formation below the Domuzdağ Complex, the presence of ophiolitic and metamorphic detritus at the top of the sequence, the south-vergent folds in the turbidites and radiolarian cherts (Tüysüz, 1985), and the northward dips of the imbricate thrusts (Fig. 3) indicate that the causative tectonic load was an accretionary complex and the emergent HP-LT metamorphic rocks. The Turonian–Coniacian age of the Kirazbaşı Formation indicates that the south-vergent thrusting started ~20 m.y. after the HP-LT metamorphism. The observation that the Kirazbaşı Formation is not deeply buried suggests that the Domuzdağ Complex had been largely exhumed by the time it was thrust over the Kirazbaşı Formation.

Kargı Complex

The Kirazbaşı Formation lies unconformably over a composite tectonic unit, the Kargı Complex, which is made up of at least two different metamorphic sequences. Garnet-amphibolite, garnet–mica schist, and marble form the upper sequence, and lower-grade metamorphic rocks the lower sequence, of the Kargı Complex (Tüysüz, 1990). The lower part of this complex is dominated by quartz–mica schists (65% of the sequence), which are locally intercalated with quartzites (10% of the sequence) and are associated with massive, thickly bedded recrystallized limestones (25% of the sequence). Rare, banded amphibolites and small lenses of metaserpentinite are present also. The recrystallized limestones occur both as interlayers within the mica schists and more commonly as large boudins in the upper parts of the sequence, interpreted as olistoliths by Tüysüz (1990). Late Carboniferous–Permian neritic foraminifers are reported from some of the recrystallized limestones (Tüysüz and Yiğitbaş, 1994). The metamorphism of the Kargı Complex is in upper greenschist facies, and is generally regarded as Permo–Triassic in age. Ustaömer and Robertson (1997) report Late Triassic (211.7 ± 18.7 Ma) K-Ar hornblende and Early Cretaceous (136.0 ± 2.9 Ma) K-Ar whole rock ages from the amphibolites of the Kargı Complex. The structural position of the Kargı Complex suggests that it is part of an exotic terrane, which collided and accreted to the Eurasian margin in the Late Cretaceous (Ustaömer and Robertson, 1997).

GEOLOGICAL EVOLUTION

Aptian–HP-LT Metamorphism and Deposition of Çağlayan Turbidites

The HP-LT metamorphism (ca. 105 Ma) is coeval with the deposition of the siliciclastic turbidites of the Çağlayan Formation along the Black Sea margin. The arc massif above the underplated Domuzdağ Complex was a major source of detritus to the West Black Sea rift (Fig. 14A). Most of the Jurassic–Cretaceous cover over the Çangaldağ Complex, as well as part of the metamorphic pile, was eroded in the Aptian–Albian. The kilometer size of the olistoliths in the Çağlayan Formation suggests that the Acısu Fault formed the main divide between the depositional and erosional realms in the Central Pontides in the Aptian.

The general absence of magmatism in the Aptian in the Central Pontides is noteworthy. Based on the magnetic isochrons in the Atlantic Ocean, the convergence between Africa and Europe is estimated to have started between 120 and 83 Ma, probably close to 95–100 Ma (Dewey et al., 1989; Rosenbaum et al., 2002). In the Aptian the subducted slab probably had not reached the depth of 150–200 km, required for arc magmatism.

Turonian–Coniacian—Exhumation of the HP-LT Metamorphic Rocks

The development of the flexural foreland basin in front of the Domuzdağ Complex indicates that the HP-LT metamorphic rocks with a leading edge of ophiolitic accretionary complex were exhumed along a thrust fault at the base and a normal fault at the top (Fig. 14B). A similar exhumation mechanism involving a basal thrust and an overlying normal fault was suggested for the Himalaya (Royden and Burchfiel, 1987), the Alps (Wheeler, 1991), the Franciscan sequence (Harms et al., 1992), and Dabie Shan in China (Hacker et al., 2000). The exhumation of the Domuzdağ Complex is constrained to a short period in the Senonian on the basis of the early Turonian–Coniacian (93–86 Ma) age of the foreland deposits and the latest Santonian–earliest Campanian (ca. 84 Ma) sedimentary cover above the HP-LT metamorphic rocks. The depth (~57 km) and age of HP-LT metamorphism (105 ± 5 Ma) give an overall vertical exhumation rate of ~3 mm per year. The forearc region in the Central Pontides was made up of Triassic subduction-accretion complexes, which were mechanically weak and contained a large number of shear zones, facilitating the emplacement of the Domuzdağ Complex. The triggering mechanism of exhumation, however, was probably the underthrusting of the Kargı microcontinent (Fig. 14B). Physical experiments have shown that underthrusting of a crustal sliver in the subduction zone may have resulted in the exhumation of the overlying slab during ongoing convergence (Chemenda et al., 1995).

The collision and accretion of the Sakarya, Kargı, and Istanbul terranes took place in the Cenomanian–Turonian (Tüysüz, 1999). The jamming of the subduction zone and continuing convergence resulted in uplift and internal deformation of the arc massif. The Cenomanian–early Turonian was a time of uplift and erosion in the Pontides. Regional shortening in this period is illustrated by the north-vergent emplacement of the ophiolitic mélange over the arc massif, possibly from the steepened and overturned accretionary complex (Dirik, 1993; Rojay, 1995; Okay and Şahintürk, 1997). A present-day analogue is the jamming of the subduction zone south of Cyprus through collision with the Eratosthenes block, a small, isolated continental terrane in the oceanic Levant basin (e.g., Robertson, 1998; Garfunkel, 1998), leading to the uplift of Cyprus above sea level.

Initiation of a New Subduction Zone—Coniacian–Santonian

The accretion of the Kargı Complex eventually resulted in the outstepping of the convergent margin and the establishment of a new subduction zone south of the Kargı Complex (Fig. 14C). The deposition of the latest Santonian–earliest Campanian pelagic limestones on the Domuzdağ Complex shows that the arc

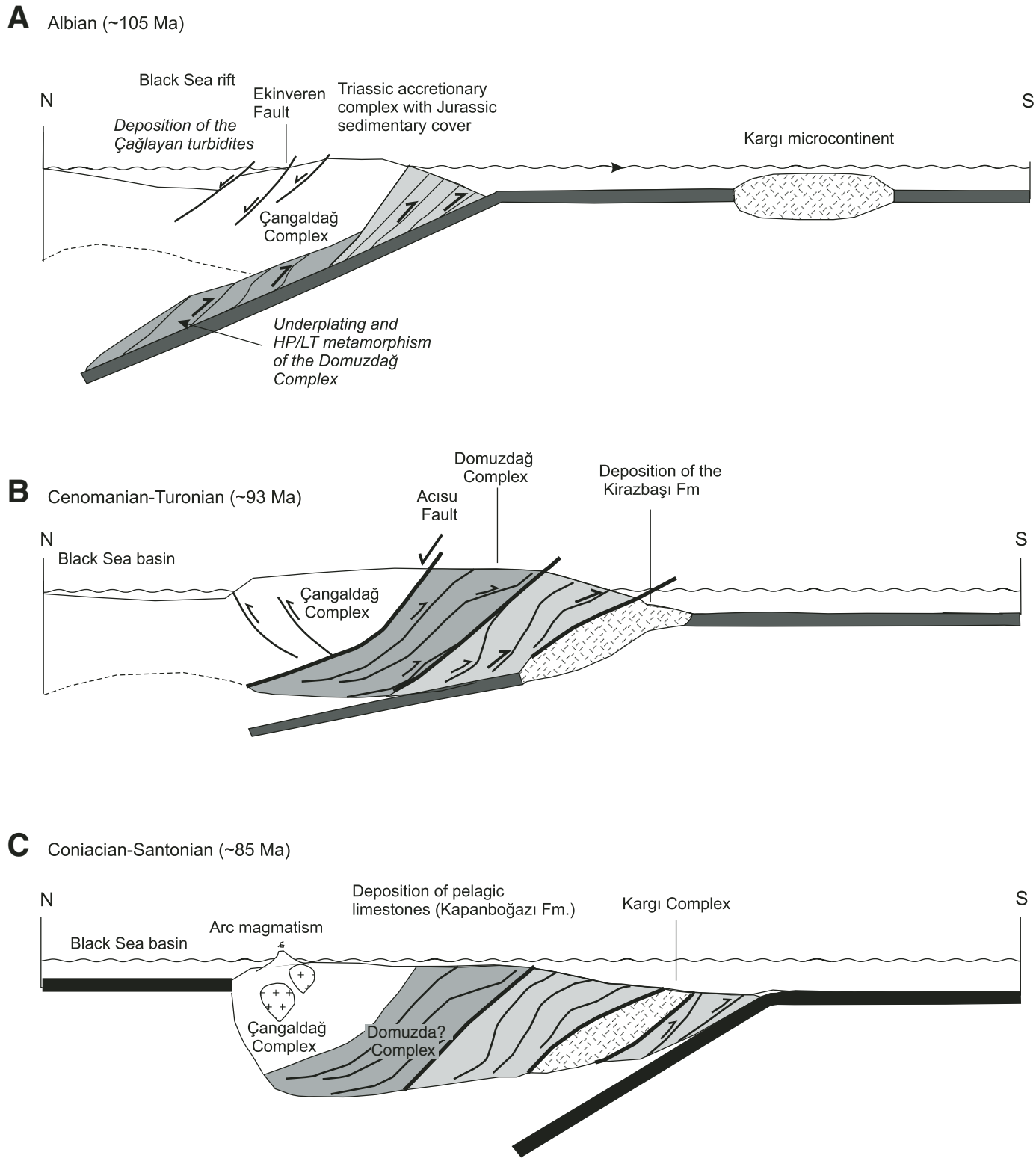

Figure 14. Sketches illustrating the tectonic evolution of the Central Pontides by outboard growth by accretion of crustal material. (A) Albian (ca. 105 Ma) HP-LT metamorphism of the underplated oceanic crust, and beginning of the rifting in the Black Sea. (B) Turonian–Coniacian (ca. 89 Ma) collision and accretion of the Kargı microcontinent and exhumation of the Domuzdağ Complex. (C) Coniacian–Santonian (ca. 85 Ma) outward thrust of the subduction zone, and the opening of the oceanic West Black Sea oceanic basin.

massif subsided below sea level by ca. 84 Ma. The regional subsidence throughout the Central and Eastern Pontides is shown by the deposition of the pelagic limestones of the Kapanboğazı Formation in the Coniacian–Santonian over a deformed substratum. This event was related to a switch from shortening to extension facilitated by the establishment of the new subduction zone. The continuing oceanic subduction also led to the first arc magmatism in the Central Pontides and to the formation of oceanic crust in the Western Black Sea basin. The pelagic limestones of the Kapanboğazı Formation are commonly interpreted as marking the breakup unconformity from rifting to the formation of the first oceanic crust (Görür et al., 1993; Robinson et al., 1996).

The absence of Cretaceous magmatic rocks within the Kargı Massif indicates that this massif was in a forearc position throughout the Santonian. Depending on the rate of subduction and on the coupling between the subducted slab and the arc massif, the forearc region underwent either uplift or subsidence. An uplift of the arc massif during the late Campanian–Maastrichtian supplied detritus for the deposition of the Gürsökü Formation. A further uplift occurred before the late Paleocene deposition of the carbonates, and the last major phase of deformation in the Gökırmak fold-and-thrust belt was in the mid-Eocene. The collision between the Central Pontides and the Kırşehir Massif began in the late Paleocene (Tüysüz and Dellaloğlu, 1992; Görür et al., 1984; Kaymakçı et al., 2003). The shortening was transmitted to the Black Sea marginal sequences in the mid-Eocene.

DISCUSSION AND CONCLUSIONS

A major part of the Central Pontides consists of Triassic and Cretaceous subduction-accretion complexes. A similar pattern of imbricated Late Cretaceous and Triassic subduction-accretion complexes, including isotopically dated Late Triassic blueschists and eclogites, was recently described from the western part of the Pontides north of Eskişehir (Okay et al., 2002) and from the Tokat Massif (Bozkurt et al., 1997). The Late Triassic Cimmeride orogeny in Anatolia was previously ascribed to the collision of a Cimmerian continental sliver with the southern margin of Eurasia (Şengör et al., 1984; Şengör, 1984). However, direct juxtaposition of the Alpide and Cimmeride subduction-accretion complexes in the Pontides leaves no room for a major Cimmeride continent. The Cimmeride orogeny in the Pontides is related to the collision and amalgamation of oceanic terranes—including oceanic plateaus, oceanic islands, and magmatic arcs—to the active margin of Eurasia in the latest Triassic and Early Jurassic (Okay, 2000; Robertson et al., 2004). It was thus an accretionary rather than a collisional orogen. The İzmir-Ankara suture is a zone of convergence during the late Paleozoic and Mesozoic and represents both the Paleo-Tethyan and Neo-Tethyan sutures.

The southern parts of the Pontides consist of lithotectonic belts that record successive outbuilding of the Laurasian continent from Triassic to Cretaceous time. In two major episodes in the Late Triassic and Late Cretaceous, the active margin of Laurasia has grown southward for >100 km through the incorporation of subduction-accretion complexes. The structure and evolution of the Pontides are similar to those of the Klamath Mountains in North America (e.g., Coleman et al., 1988) and to the Altaids in Central Asia (Şengör et al., 1993) rather than to the collisional orogens of the Western Alps or Himalaya. However, the Pontides differs from these other regions by the general scarcity of arc magmatism, possibly because the subducted oceanic lithosphere was not wide or the subduction angle was too shallow to generate arc magmas.

The Central Pontides contains one of the earliest records of the Alpide convergence in the Eastern Mediterranean in the Albian (ca. 105 Ma) HP-LT metamorphism. The Cretaceous–Tertiary sedimentary sequences indicate that the HP-LT metamorphic rocks were exhumed in the Turonian–Coniacian at ca. 86 Ma in a forearc setting in a convergent subduction system. The exhumation of the HP-LT metamorphic complex was guided by a basal thrust, which led to the development of a flexural foreland basin in the south. The upper tectonic contact of the HP-LT metamorphic complex was a shear zone with a normal sense of movement. Oceanic subduction continued in the Central Pontides at least until the Paleocene, and the exhumation of the HP-LT metamorphic rocks predated the collision by ~25 m.y. The exhumation of the HP-LT metamorphic rocks was probably triggered by the underthrusting of a small continental terrane (Fig. 14B).

HP-LT metamorphic complexes, backarc basins, and detachment faults are common in the Mediterranean region; their temporal and causal relation are controversial (e.g., Avigad et al., 1997; Gautier, 2000). In the Central Pontides the Acısu detachment fault forms the southern depositional limit of the Cretaceous–Eocene Black Sea marginal sequence. During its main phase of activity in the Albian–Santonian, the Acısu Fault could have created the space for the deposition of the turbidites of the Çağlayan Formation. However, any causal link between the structures responsible for the exhumation of the HP-LT metamorphic rocks and those for the development of oceanic crust in the West Black Sea basin is difficult to establish because of the discrepancy in their scale (cf. Fig. 1).

The Central Pontides has been an important region in the development of the concepts related to the Cimmeride evolution in the Eastern Mediterranean realm (Şengör et al., 1984; Yılmaz and Şengör, 1985; Tüysüz, 1990; Ustaömer and Robertson, 1997; Robertson et al., 2004). In all these models the HP-LT metamorphic rocks, including the Domuzdağ Complex and the Elekdağ lherzolite, were regarded as pre-Jurassic units that represent the main Paleo-Tethyan ocean. Their Alpide rather than Cimmeride age requires modification to the Paleo-Tethyan models. One implication of the new data is that there is no evidence for the existence of a Late Triassic–Liassic Küre basin, which was modeled to have opened north of the main Paleo-Tethys (Ustaömer and Robertson, 1997; Stampfli and Borel, 2002; Robertson et al., 2004). The Küre basin is a forearc to trench basin above the northward dipping Paleo-Tethyan subduction zone, close to the Eurasian margin.

HP-LT metamorphic rocks of Precambrian (Candan et al., 2001), Late Triassic (Okay and Monié, 1997; Okay et al., 2002), mid-Cretaceous (this study), Late Cretaceous (Sherlock et al., 1999), and Eocene ages (Oberhänsli et al., 1998) occur within the relatively confined area of Anatolia and attest to its location along active plate boundaries throughout the Phanerozoic. Although oceanic subduction was a steady-state process during much of the Cretaceous along the Pontide margin, accretion of the subduction complexes to the continental margin was episodic and happened at different times in different segments of the margin. The triggering mechanism for the accretion of the subduction complexes was collision of small continental or oceanic fragments with the subduction zone.

APPENDIX: ANALYTICAL TECHNIQUES FOR ISOTOPIC DATING

For the Ar-Ar analyses, the eclogite sample was prepared as a polished section, 300 μm in thickness, and was removed from the glass slide and cleaned in alternate acetone and deionized water. A 5 mm^2 piece was selected for irradiation and removed with a scalpel, which was packaged in aluminum foil. The sample was irradiated at the Risø reactor (Denmark) for 13 h. Neutron flux was monitored using GA1550 biotite (with an age of 98.8 ± 0.5 Ma), with a *J* value of 0.0065 ± 0.0000325. Results were corrected for blanks, ^{37}Ar decay, and neutron-induced interference reactions. The following correction factors were used: $(^{39}Ar/^{37}Ar)_{Ca} = 0.00067$, $(^{36}Ar/^{37}Ar)_{Ca} = 0.000255$, and $(^{40}Ar/^{39}Ar)_{K} = 0.048$; these were

based on analyses of Ca and K salts. In situ laser spot analyses were performed on micas within the thick section. These were carried out using a 1064 nm CW Nd-YAG, with a beam size of ca. 50 μm. Extracted gases were analyzed using a fully automated MAP 215–50 noble gas mass spectrometer.

For Rb-Sr dating, mineral separation was performed by heavy liquids, magnetic separation, and handpicking. Sample splits of ~50–100 mg were dissolved in Teflon beakers (perfluoralkoxy) with HF and $HClO_4$. For isotope analyses, Sr and light rare-earth elements were isolated on quartz columns by conventional ion exchange chromatography with a 5-mL resin bed of Bio Rad AG 50W-X12, 200–400 mesh. Sr was loaded with a Ta-HF activator on preconditioned W filaments and was measured in single-filament mode. The $^{87}Sr/^{86}Sr$ ratios were normalized to $^{86}Sr/^{88}Sr = 0.1194$. The total procedure blank for Sr and Rb is less than 0.5 ng. Age determinations are based on the ^{87}Rb decay constant of 1.42×10^{-11} yr^{-1} as recommended by Steiger and Jaeger (1977). Isotope analyses were made on a Finnigan MAT 262 mass spectrometer in Tübingen. Analyses of Sr standards (National Bureau of Standards NBS 987) gave $^{87}Sr/^{86}Sr$ ratios 0.710259 ± 0.000010 (2σ of 28 analyses). The input error for age calculations is 1% (2σ) for the $^{87}Rb/^{86}Sr$ ratios and 0.003% (2σ) for the $^{87}Sr/^{86}Sr$ ratios. Regression lines were calculated by the least-squares cubic method of York (1969) using the ISOPLOT software of Ludwig (1988) and Wendt (1984).

ACKNOWLEDGMENTS

We thank TÜBİTAK (grant YDABAG 101Y032), ITU Research Fund (grant 2020), and TUBA for financial support. We gratefully acknowledge the paleontological determinations of Ercüment Sirel for the Paleocene–Eocene sequences. Heinz-Jürgen Bernhardt is thanked for help with the microprobe and Kenan Akbayram for assistance in the field. The manuscript was considerably improved through the thoughtful comments of GSA editors John Wakabayashi, Laurent Jolivet, and John Platt.

REFERENCES CITED

Akıncı, Ö.T., 1984, The Eastern Pontide volcano-sedimentary belt and associated massive sulphide deposits, *in* Dixon, J.E., and Robertson, A.H.F., eds., The geological evolution of the Eastern Mediterranean: Geological Society [London] Special Publication 17, p. 415–428.

Aksay, A., Pehlivan, Ş., Gedik, İ., Bilginer, E., Duru, M., Akbaş, B., and Altun, İ., 2002, Geological map of Turkey, Zonguldak sheet: Ankara, Maden Tetkik ve Arama Genel Müdürlüğü, scale 1:500,000.

Altherr, R., Topuz, G., Marschall, H., Zack, T., and Ludwig, T., 2004, Evolution of a tourmaline-bearing lawsonite eclogite from the Elekdag area (Central Pontides, N Turkey): Evidence for infiltration of slab-derived B-rich fluids during exhumation: Contributions to Mineralogy and Petrology, v. 148, p. 409–425.

Aoki, K., Fujina, K., and Akaoji, M., 1976, Titanochondrodite and titanoclinohumite derived from the upper mantle in the Buell Park kimberlite, Arizona, USA: Contributions to Mineralogy and Petrology, v. 56, p. 243–253, doi: 10.1007/BF00466824.

Arslan, M., Tuysuz, N., Korkmaz, S., and Kurt, H., 1997, Geochemistry and petrogenesis of the eastern Pontide volcanic rocks, northeast Turkey: Chemie der Erde—Geochemistry, v. 57, p. 157–187.

Avigad, D., Garfunkel, Z., Jolivet, L., and Azanon, J.M., 1997, Back arc extension and denudation of Mediterranean eclogites: Tectonics, v. 16, p. 924–941, doi: 10.1029/97TC02003.

Aydın, M., Şahintürk, Ö., Serdar, H.S., Özçelik, Y., Akarsu, İ., Üngör, A., Çokuğraş, R., and Kasar, S., 1986, The geology of the region between Ball dağ and Çangaldağ Kastamonu): Türkiye Jeoloji Kurumu Bülteni, v. 29, p. 1–16.

Aydın, M., Demir, O., Özçelik, Y., Terzioğlu, N., and Satır, M., 1995, A geological revision of İnebolu, Devrekani, Ağlı and Küre areas: New observations in Paleo-Tethys–Neo-Tethys sedimentary successions, *in* Erler, A., et al., eds., Geology of the Black Sea region: Ankara, Maden Tetkik ve Arama Genel Müdürlüğü, p. 33–38.

Boccaletti, M., Gocev, P., and Manetti, P., 1974, Mesozoic isopic zones in the Black Sea region: Societa Geologica Italiana Bollettino, v. 93, p. 547–565.

Bozkurt, E., Holdsworth, B.K., and Koçyiğit, A., 1997, Implications of Jurassic chert identified in the Tokat Complex, northern Turkey: Geological Magazine, v. 134, p. 91–97, doi: 10.1017/S0016756897006419.

Çamur, M.Z., Güven, İ.H., and Er, M., 1996, Geochemical characteristics of the Eastern Pontide volcanics, Turkey: An example of multiple volcanic cycles in the arc evolution: Turkish Journal of Earth Sciences, v. 5, p. 123–144.

Candan, O., Dora, O.Ö., Oberhänsli, R., Çetinkaplan, M., Partzsch, J.H., Warkus, F.C., and Dürr, S., 2001, Pan-African high-pressure metamorphism in the Precambrian basement of the Menderes Massif, western Anatolia, Turkey: International Journal of Earth Sciences, v. 89, p. 793–811, doi: 10.1007/s005310000097.

Caron, M., 1985, Cretaceous planktic foraminifera, *in* Bolli, H.M., et al., eds., Plankton stratigraphy: Cambridge, UK, Cambridge University Press, v. 1, p. 17–86.

Carpenter, M.A., 1980, Mechanisms of exsolution in sodic pyroxenes: Contributions to Mineralogy and Petrology, v. 71, p. 289–300, doi: 10.1007/BF00371671.

Channell, J.E.T., Tüysüz, O., Bektas, O., and Sengör, A.M.C., 1996, Jurassic–Cretaceous paleomagnetism and paleogeography of the Pontides (Turkey): Tectonics, v. 15, p. 201–212, doi: 10.1029/95TC02290.

Chemenda, A.I., Mattauer, M., Malavieille, J., and Bokun, A.N., 1995, A mechanism for syn-collisional rock exhumation and associated normal faulting—Results from physical modeling: Earth and Planetary Science Letters, v. 132, p. 225–232, doi: 10.1016/0012-821X(95)00042-B.

Chopin, C., 1981, Talc-phengite: A widespread assemblage in high-grade pelitic blueschists of the Western Alps: Journal of Petrology, v. 22, p. 628–650.

Coleman, R.G., Mortimer, N., Donato, M.M., Manning, C.E., and Hill, L.B., 1988, Tectonic and regional metamorphic framework of the Klamath Mountains–Sierra Nevada geological terrane, *in* Ernst, W.G., ed., Metamorphism and crustal evolution of the western United States: Englewood Cliffs, New Jersey, Prentice Hall, p. 1061–1097.

Coney, P.J., Jones, D.L., and Monger, J.W.H., 1980, Cordilleran suspect terranes: Nature, v. 288, p. 329–333, doi: 10.1038/288329a0.

DeCelles, P.G., and Giles, K.A., 1996, Foreland basin systems: Basin Research, v. 8, p. 105–123, doi: 10.1046/j.1365-2117.1996.01491.x.

Dercourt, J., Zonenshain, L.P., Ricou, L.-E, Kazmin, V.G., Le Pichon, X., Knipper, A.L., Grandjacquet, C., Sbortshikov, I.M., Geyssant, J., Lepvrier, C., Perchersky, D.H., Boulin, J., Sibuet, J.-C., Savostin, L.A., Sorokhtin, O., Westphal, M., Bazhenov, M.L., Lauer, J.P., and Biju-Duval, B., 1986, Geological evolution of the Tethys belt from the Atlantic to the Pamirs since the Lias: Tectonophysics, v. 123, p. 241–315.

Dewey, J.F., Helman, M.L., Turco, E., Hutton, D.H.W., and Knott, S.D., 1989, Kinematics of the western Mediterranean, *in* Coward, M.P., et al., eds., Alpine tectonics: Geological Society [London] Special Publication 45, p. 265–283.

Dilek, Y., 2003, Ophiolite concept and its evolution, *in* Dilek, Y., and Newcomb, S., eds., Ophiolite concept and the evolution of geological thought: Geological Society of America Special Paper 373, p. 1–16.

Dirik, K., 1993, Geological history of the northward arched segment of the North Anatolian Transform fault zone: Geological Journal, v. 28, p. 251–266.

Ellis, D.J., and Green, D.H., 1979, An experimental study of the effect of Ca upon garnet-clinopyroxene Fe-Mg exchange equilibria: Contributions to Mineralogy and Petrology, v. 71, p. 13–22, doi: 10.1007/BF00371878.

El-Shazly, A.K., and Liou, J.G., 1991, Glaucophane chloritoid-bearing assemblages from NE Oman: Petrologic significance and a petrogenetic grid for high P metapelites: Contributions to Mineralogy and Petrology, v. 107, p. 180–201, doi: 10.1007/BF00310706.

Eren, R.H., 1979, Geological and petrological study of the metamorphic rocks in the Kastamonu-Taşköprü region [Ph.D. thesis]: Istanbul, Istanbul Technical University, 143 p. (in Turkish).

Ernst, W.G., 1984, Californian blueschists, subduction and the significance of tectonostratigraphic terranes: Geology, v. 12, p. 436–440, doi: 10.1130/0091-7613(1984)12<436:CBSATS>2.0.CO;2.

Evans, B.W., 1990, Phase relations of epidote-blueschists: Lithos, v. 25, p. 3–23, doi: 10.1016/0024-4937(90)90003-J.

Evans, B.W., and Trommsdorff, V., 1983, Fluorine hydroxyl titanian clinohumite in alpine recrystallised garnet peridotite: Compositional controls and petrological significance: American Journal of Science, v. 283-A, p. 355–369.

Faryad, S.W., 1995, Petrology and phase-relations of low-grade high-pressure metasediments from the Meliata unit (west Carpathians, Slovakia): European Journal of Mineralogy, v. 7, p. 71–87.

Forbes, R.B., Evans, B.W., and Thurston, S.P., 1984, Regional progressive high-pressure metamorphism, Seward Peninsula, Alaska: Journal of Metamorphic Geology, v. 2, p. 43–54.

Garfunkel, Z., 1998, Constraints on the origin and history of the Eastern Mediterranean basin: Tectonophysics, v. 298, p. 5–35, doi: 10.1016/S0040-1951(98)00176-0.

Gautier, P., 2000, Comment on "Back arc extension and denudation of Mediterranean eclogites": Tectonics, v. 19, p. 406–409, doi: 10.1029/1999TC900068.

Gedik, A., and Korkmaz, S., 1984, Geology and petroleum potential of the Sinop basin: Jeoloji Mühendisliği, v. 19, p. 53–79.

Görür, N., 1988, Timing of opening of the Black Sea basin: Tectonophysics, v. 147, p. 247–262, doi: 10.1016/0040-1951(88)90189-8.

Görür, N., and Tüysüz, O., 1997, Petroleum geology of the southern continental margin of the Black Sea, *in* Robinson, A.G., ed., Regional and petroleum geology of the Black Sea and surrounding region: American Association of Petroleum Geologists Memoir 68, p. 241–254.

Görür, N., Oktay, F.Y., Seymen, İ., and Şengör, A.M.C., 1984, Paleotectonic evolution of the Tuzgölü basin complex, Central Anatolia: Sedimentary record of a Neo-Tethyan closure, *in* Dixon, J.E., and Robertson, A.H.F., eds., The geological evolution of the Eastern Mediterranean: Geological Society [London] Special Publication 17, p. 455–466.

Görür, N., Tüysüz, O., Aykol, A., Sakınç, M., Yiğitbaş, E., and Akkök, R., 1993, Cretaceous red pelagic carbonates of northern Turkey: Their place in the opening history of the Black Sea: Eclogae Geologica Helvetica, v. 86, p. 819–838.

Görür, N., Monod, O., Okay, A.I., Şengör, A.M.C., Tüysüz, O., Yiğitbaş, E., Sakınç, M., and Akkök, R., 1997, Palaeogeographic and tectonic position of the Carboniferous rocks of the western Pontides (Turkey) in the frame of the Variscan belt: Bulletin de la Société Géologique de France, v. 168, p. 197–205.

Gradstein, F.M., Ogg, J.G., Smith, A.G., Bleeker, W., and Lourens, L.J., 2004, A new geological time scale with special reference to Precambrian and Neogene: Episodes, v. 26, p. 83–100.

Hacker, B.R., Ratschbacher, L., Webb, L., McWilliams, M.O., Ireland, T., Calvert, A., Dong, S.W., Wenk, H.R.,

and Chateigner, D., 2000, Exhumation of ultrahigh-pressure continental crust in east central China: Late Triassic–Early Jurassic tectonic unroofing: Journal of Geophysical Research, v. 105, p. 13,339–13,364, doi: 10.1029/2000JB900039.

Harms, T., Jayko, A.S., and Blake, M.C., 1992, Kinematic evidence for extensional unroofing of the Franciscan complex along the Coast Range fault, northern Diablo Range, California: Tectonics, v. 11, p. 228–241.

Holland, T.J.B., and Powell, R., 1998, An internally consistent thermodynamic data set for phases of petrological interest: Journal of Metamorphic Geology, v. 16, p. 309–343, doi: 10.1111/j.1525-1314.1998.00140.x.

Irwin, W.P., 1981, Tectonic accretion of the Klamath Mountains, *in* Ernst, W.G., ed., The geotectonic development of California (Rubey Volume 1): Englewood Cliffs, New Jersey, Prentice Hall, p. 29–49.

Jäger, E., Niggli, E., and Wenk, E., 1967, Rb-Sr Altersbestimmungen an Glimmern der Zentralalpen: Beiträge zu der geologische Karte der Schweiz, NF 134, 67 p.

Kaya, O., and Mostler, H., 1992, A Middle Triassic age for low-grade greenschist facies metamorphic sequence in Bergama (Izmir), western Turkey: The first paleontological age assignment and structural-stratigraphic implications: Newsletter for Stratigraphy, v. 26, p. 1–17.

Kaymakçı, N., Stanley, H.W., and Vandijk, P.M., 2003, Kinematic and structural development of the Çankırı Basin (Central Anatolia, Turkey): A paleostress inversion study: Tectonophysics, v. 364, p. 85–113, doi: 10.1016/S0040-1951(03)00043-X.

Koçyiğit, A., 1991, An example of an accretionary forearc basin from northern Central Anatolia and its implications for the history of subduction of Neo-Tethys in Turkey: Geological Society of America Bulletin, v. 103, p. 22–36, doi: 10.1130/0016-7606(1991)103<0022:AEOAAF>2.3.CO;2.

Kozur, H., Aydın, M., Demir, O., Yakar, H., Göncüoğlu, M.C., and Kuru, F., 2000, New stratigraphic and palaeogeographic results from the Palaeozoic and early Mesozoic of the Middle Pontides (northern Turkey) in the Azdavay, Devrekani, Küre and İnebolu areas: Implications for the Carboniferous–Early Cretaceous geodynamic evolution and some related remarks to the Karakaya oceanic rift basin: Geologica Croatica, v. 53, p. 209–268.

Ludwig, K.R., 1988, A plotting and regression program for radiogenic-isotope data for IBM-PC compatible computers: U.S. Geological Survey Open-File Report 88-557, 16 p.

Manetti, P., Peccerillo, A., Poli, G., and Corsini, F., 1983, Petrochemical constraints on the models of Cretaceous–Eocene tectonic evolution of the Eastern Pontic chain (Turkey): Cretaceous Research, v. 4, p. 159–172, doi: 10.1016/0195-6671(83)90047-2.

Milch, L., 1907, Über Glaukophan und Glaukophan-gesteine vom Elek Dağ (nördliches Kleinasien) mit Beitragen zur Kenntnis der chemischen Beziehungen basischer Glaukophangesteine: Neues Jahrbuch für Mineralogie, Geologie und Palaeontologie, Festband, p. 348–396.

Oberhänsli, R., Monie, P., Candan, O., Warkus, F.C., Partzsch, J.H., and Dora, O.Ö., 1998, The age of blueschist metamorphism in the Mesozoic cover series of the Menderes Massif: Schweizerische Mineralogische und Petrographische Mitteilungen, v. 78, p. 309–316.

Okay, A.I., 1994, Sapphirine and Ti-clinohumite in ultrahigh-pressure garnet-pyroxenite and eclogite from Dabie Shan, China: Contributions to Mineralogy and Petrology, v. 116, p. 145–155, doi: 10.1007/BF00310696.

Okay, A.I., 2000, Was the Late Triassic orogeny in Turkey caused by the collision of an oceanic plateau?, *in* Bozkurt, E., et al., eds., Tectonics and magmatism in Turkey and surrounding area: Geological Society [London] Special Publication 173, p. 25–41.

Okay, A.I., and Göncüoğlu, M.C., 2004, Karakaya Complex: A review of data and concepts: Turkish Journal of Earth Sciences, v. 13, p. 77–95.

Okay, A.I., and Monié, P., 1997, Early Mesozoic subduction in the Eastern Mediterranean: Evidence from Triassic eclogite in northwest Turkey: Geology, v. 25, p. 595–598, doi: 10.1130/0091-7613(1997)025<0595:EMSITE>2.3.CO;2.

Okay, A.I., and Şahintürk, Ö., 1997, Geology of the Eastern Pontides, *in* Robinson, A.G., ed., Regional and petroleum geology of the Black Sea and surrounding region: American Association of Petroleum Geologists Memoir 68, p. 291–311.

Okay, A.I., and Tüysüz, O., 1999, Tethyan sutures of northern Turkey, *in* Durand, B., Jolivet, L., Horváth, F., and Séranne, M., The Mediterranean basins: Tertiary extension within the Alpine orogen: Geological Society [London] Special Publication 156, p. 475–515.

Okay, A.I., Monod, O., and Monié, P., 2002, Triassic blueschists and eclogites from northwest Turkey: Vestiges of the Paleo-Tethyan subduction: Lithos, v. 64, p. 155–178, doi: 10.1016/S0024-4937(02)00200-1.

Özcan, E., and Özkan-Altıner, S., 1999, The genera *Lepidorbitoides* and *Orbitoides:* Evolution and stratigraphic significance in some Anatolian basins: Geological Journal, v. 34, p. 275–286, doi: 10.1002/(SICI)1099-1034(199907/09)34:3<275::AID-GJ827>3.0.CO;2-J.

Özkan-Altıner, S., and Özcan, E., 1999, Upper Cretaceous planktonic foraminiferal biostratigraphy from NW Turkey: Calibration of the stratigraphic ranges of larger benthonic foraminifera: Geological Journal, v. 34, p. 287–301, doi: 10.1002/(SICI)1099-1034(199907/09)34:3<287::AID-GJ828>3.0.CO;2-B.

Patrick, B.E., and Evans, B.W., 1989, Metamorphic evolution of the Seward Peninsula blueschist terrane: Journal of Petrology, v. 30, p. 531–555.

Pelin, S., 1977, Geological study of the area southeast of Alucra (Giresun) with special reference to its petroleum potential: Trabzon, Turkey, Karadeniz Teknik Üniversitesi Publication 87, 103 p. (in Turkish).

Pelin, S., Özsayar, T., Gedikoğlu, A., and Tülümen, E., 1982, The origin of the Upper Cretaceous red biomicrites in the Eastern Pontides: Karadeniz Üniversitesi Yer Bilimleri Dergisi Jeoloji, v. 2, p. 69–80.

Pickett, E.A., and Robertson, A.H.F., 2004, Significance of the volcanogenic Nilüfer Unit and related components of the Triassic Karakaya Complex for Tethyan subduction/accretion processes in NW Turkey: Turkish Journal of Earth Sciences, v. 13, p. 97–144.

Powell, R., and Holland, T.J.B., 1988, An internally consistent thermodynamic dataset with uncertainties and correlations: 3. Application methods, worked examples and a computer program: Journal of Metamorphic Geology, v. 6, p. 173–204.

Premoli Silva, I., and Sliter, W.V., 1994, Cretaceous planktonic foraminiferal biostratigraphy and evolutionary trends from the Bottaccione section, Gubbio, Italy: Palaeontographia Italica, v. 82, p. 1–89.

Purdy, J.W., and Jäger, E., 1976, K-Ar ages on rock-forming minerals from the Central Alps: Padova [Padua], Memoires Institute Geologica Mineralogica, Universita Padova, v. 30, 31 p.

Robaszynski, F., Gonzalez Donoso, J.M., Linares, D., Amedro, F., Caron, M., Dupuis, C., Dhondt, A.V., and Gartner, S., 2000, Le Crétace Supérieur de la région de Kalaat Senan, Tunusie Centrale: Litho-Biostratigraphie intérée: Zones d'ammonites, de foraminifeeres planctoniques et de nannofossiles du Turonien Supérieur au Maastrichtien: Bull. Centres Rech. Explor.-Prod: Elf-Aquitaine, v. 22, p. 359–490.

Robertson, A.H.F., 1998, Tectonic significance of the Eratosthenes Seamount: A continental fragment in the process of collision with a subduction zone in the eastern Mediterranean (Ocean Drilling Program Leg 160): Tectonophysics, v. 298, p. 63–82, doi: 10.1016/S0040-1951(98)00178-4.

Robertson, A.H.F., Ustaömer, T., Pickett, E., Collins, A., Andrew, T., and Dixon, J.E., 2004, Testing models of Late Palaeozoic–Early Mesozoic orogeny in Western Turkey: Support for an evolving open-Tethys model: Geological Society [London] Journal, v. 161, p. 501–511.

Robinson, A.G., Banks, C.J., Rutherford, M.M., and Hirst, J.P.P., 1995, Stratigraphic and structural development of the Eastern Pontides, Turkey: Geological Society [London] Journal, v. 152, p. 861–872.

Robinson, A.G., Rudat, J.H., Banks, C.J., and Wiles, R.L.F., 1996, Petroleum geology of the Black Sea: Marine and Petroleum Geology, v. 13, p. 195–223, doi: 10.1016/0264-8172(95)00042-9.

Rojay, B., 1995, Post-Triassic evolution of Central Pontides: Evidence from Amasya region, northern Anatolia: Geologica Romana, v. 31, p. 329–350.

Rojay, B., and Altıner, D., 1998, Middle Jurassic–Lower Cretaceous biostratigraphy in the Central Pontides (Turkey): Remarks on paleogeography and tectonic evolution: Rivista Italiana Paleontologia e Stratigrafia, v. 104, p. 167–180.

Rosenbaum, G., Lister, G.S., and Duboz, C., 2002, Relative motions of Africa, Iberia and Europe during Alpine orogeny: Tectonophysics, v. 359, p. 117–129, doi: 10.1016/S0040-1951(02)00442-0.

Royden, L., and Burchfiel, B.C., 1987, Thin-skinned extension within the convergent Himalayan region: Gravitational collapse of a Miocene topographic front: Geological Society [London] Special Publication 28, p. 611–619.

Schliestedt, M., 1986, Eclogite-blueschist relationships as evidenced by mineral equilibrium in the high pressure metabasic rocks of Sifnos (Cycladic Islands), Greece: Journal of Petrology, v. 27, p. 1439–1459.

Şengör, A.M.C., 1984, The Cimmeride orogenic system and the tectonics of Eurasia: Geological Society of America Special Paper 195, 82 p.

Şengör, A.M.C., 1987, Tectonics of the Tethysides: Orogenic collage development in a collisional setting: Annual Review of Earth and Planetary Sciences, v. 15, p. 213–244, doi: 10.1146/annurev.ea.15.050187.001241.

Şengör, A.M.C., Yılmaz, Y., and Sungurlu, O., 1984, Tectonics of the Mediterranean Cimmerides: Nature and evolution of the western termination of Palaeo-Tethys, *in* Dixon, J.E., and Robertson, A.H.F., eds., The geological evolution of the Eastern Mediterranean: Geological Society [London] Special Publication 17, p. 77–112.

Şengör, A.M.C., Natal'in, B.A., and Burtman, V.S., 1993, Evolution of the Altaid tectonic collage and Palaeozoic crustal growth in Eurasia: Nature, v. 364, p. 299–307, doi: 10.1038/364299a0.

Sherlock, S., Kelley, S.P., Inger, S., Harris, N., and Okay, A.I., 1999, ^{40}Ar-^{39}Ar and Rb-Sr geochronology of high-pressure metamorphism and exhumation history of the Tavsanli Zone, NW Turkey: Contributions to Mineralogy and Petrology, v. 137, p. 46–58, doi: 10.1007/s004100050581.

Stampfli, G.M., and Borel, G.D., 2002, A plate tectonic model for the Paleozoic and Mesozoic constrained by dynamic plate boundaries and restored synthetic oceanic isochrons: Earth and Planetary Science Letters, v. 196, p. 17–33, doi: 10.1016/S0012-821X(01)00588-X.

Steiger, R.H., and Jaeger, E., 1977, Subcommission on geochronology: Convention on the use of decay constants in geo- and cosmochronology: Earth and Planetary Science Letters, v. 36, p. 359–362, doi: 10.1016/0012-821X(77)90060-7.

Theye, T., and Seidel, E., 1991, Petrology of low-grade high-pressure metapelites from the External Hellenides (Crete, Peloponnese): A case study with attention to sodic minerals: European Journal of Mineralogy, v. 3, p. 343–366.

Toumarkine, M., and Lutherbacher, H., 1985, Paleocene and Eocene planktic foraminifera, *in* Bolli, H.M., et al., eds., Plankton stratigraphy: Cambridge, UK, Cambridge University Press, v. 1, p. 87–154.

Tüysüz, O., 1985, The distinction and petrological study of the tectonic units in the Kargı Massif [Ph.D. thesis]: Istanbul, Istanbul Üniversitesi, Fen Bilimleri Enstitüsü, 431 p. (in Turkish).

Tüysüz, O., 1990, Tectonic evolution of a part of the Tethyside orogenic collage: The Kargı Massif, northern Turkey: Tectonics, v. 9, p. 141–160.

Tüysüz, O., 1993, A geotraverse from the Black Sea to the Central Anatolia: Tectonic evolution of the northern Neo-Tethys: Türkiye Petrol Jeologları Derneği Bülteni, v. 5, p. 1–33.

Tüysüz, O., 1998, Digital geologic map of Turkey: Sinop sheet: Istanbul, Istanbul Technical University, scale 1:500,000.

Tüysüz, O., 1999, Geology of the Cretaceous sedimentary basins of the Western Pontides: Geological Journal, v. 34, p. 75–93, doi: 10.1002/(SICI)1099-1034(199901/06)34:1/2<75::AID-GJ815>3.0.CO;2-S.

Tüysüz, O., and Dellaloğlu, A.A., 1992, The tectonic units of the Çankırı basin and its geological evolution:

Proceedings of 9th Petroleum Congress of Turkey, p. 1–17 (in Turkish).

Tüysüz, O., and Yiğitbaş, E., 1994, The Karakaya basin: A Palaeo-Tethyan marginal basin and its age of opening: Acta Geologica Hungarica, v. 37, p. 327–350.

Uğuz, M.F., Sevin, M., Duru, M., 2002, Geological map of Turkey, Sinop sheet: Ankara, Maden Tetkik ve Arama Genel Müdürlüğü, scale 1:500,000.

Ustaömer, T., and Robertson, A.H.F., 1994, Late Paleozoic marginal basin and subduction-accretion: The Paleo-tethyan Küre Complex, Central Pontides, northern Turkey: Geological Society [London] Journal, v. 151, p. 291–305.

Ustaömer, T., and Robertson, A.H.F., 1997, Tectonic-sedimentary evolution of the North-Tethyan margin in the Central Pontides of northern Turkey, *in* Robinson, A.G., ed., Regional and petroleum geology of the Black Sea and surrounding region: American Association of Petroleum Geologists Memoir 68, p. 255–290.

Ustaömer, T., and Robertson, A.H.F., 1999, Geochemical evidence used to test alternative plate tectonic models for the pre–Upper Jurassic (Palaeotethyan) units in the Central Pontides, N Turkey: Geological Journal, v. 34, p. 25–53, doi: 10.1002/(SICI)1099-1034(199901/06)34:1/2<25::AID-GJ813>3.0.CO;2-C.

Wakabayashi, J., 1999, The Franciscan: California's classic subduction complex, *in* Moores, E.M., et al., eds., Classic Cordilleran concepts: A view from California: Geological Society of America Special Paper 373, p. 111–121.

Wendt, I., 1984, A three dimensional U-Pb discordia plane to evaluate samples with common lead of unknown isotopic composition: Isotopic Geoscience, v. 2, p. 1–12.

Wheeler, J., 1991, Structural evolution of a subducted continental sliver: The northern Dora Maira massif, Italian Alps: Geological Society [London] Journal, v. 148, p. 1101–1114.

Yiğitbaş, E., Tüysüz, O., and Serdar, H.S., 1990, The geological characteristics of the Late Cretaceous active margin in the Central Pontides: Proceedings of 8th Petroleum Congress of Turkey, p. 141–151 (in Turkish).

Yılmaz, O., 1980, Tectonics and the lithostratigraphic units of the northeastern part of the Daday-Devrakani Massif: Yerbilimleri, v. 5–6, p. 101–135.

Yılmaz, O., 1983, Mineralogical-petrographical study of the Çangal metaophiolite and its metamorphic conditions: Yerbilimleri, v. 10, p. 45–58.

Yılmaz, O., and Boztuğ, D., 1986, Kastamonu granitoid belt of northern Turkey: First arc plutonism product related to the subduction of the Paleo-Tethys: Geology, v. 14, p. 179–183, doi: 10.1130/0091-7613(1986)14<179:KGBONT>2.0.CO;2.

Yılmaz, Y., and Şengör, A.M.C., 1985, Palaeo-Tethyan ophiolites in northern Turkey: Petrology and tectonic setting: Ofioliti, v. 10, p. 485–504.

Yılmaz, Y., Tüysüz, O., Yiğitbaş, E., Genç, Ş.C., and Şengör, A.M.C., 1997, Geology and tectonic evolution of the Pontides, *in* Robinson, A.G., ed., Regional and petroleum geology of the Black Sea and surrounding region: American Association of Petroleum Geologists Memoir 68, p. 183–226.

York, D., 1969, Least-square fitting with a straight line with correlated errors: Earth and Planetary Science Letters, v. 5, p. 320–324, doi: 10.1016/S0012-821X(68)80059-7.

Manuscript Received 22 November 2005
Revised Manuscript Received 3 March 2006
Manuscript Accepted 19 March 2006

Printed in the USA

Statement of Ownership, Management, and Circulation
(Required by Title 39 U.S.C. 4369)

The Geological Society of America Bulletin (Publication No. 0016-7606) is published bi-monthly by The Geological Society of America, Inc., (GSA) with headquarters and offices at 3300 Penrose Place, Boulder, Colorado 80301 U.S.A.; and mailing address of Post Office Box 9140, Boulder, Colorado 80301-9140 U.S.A. The Publisher is Jon Olsen; offices and mailing addresses are the same as above. The annual subscription prices are: GSA Members $82; GSA Associate-Student Members $40; non-members $600. The publication is wholly owned by The Geological Society of America, Inc., a not-for-profit, charitable corporation. No known stockholder holds 1 percent or more of the total stock. CEDE & Company, 55 Water Street, New York, NY 10041, holds all outstanding bonds; there are no known mortgagees or holders of other securities. The purpose, function, and nonprofit status of The Geological Society of America, Inc., has not changed during the preceding twelve months. The average number of copies of each issue during the preceding twelve months and the actual number of copies published nearest to the filing date (September 2006 issue) are noted at right.

This information taken from PS Form 3526, signed 17 August 2006 by the Publisher, Jon Olsen, and filed with the United States Postal Service in Boulder, Colorado.

Item No. from PS Form 3526	Extent and Nature of Circulation	Avg. No. Copies Each Issue in past 12 Months	Actual No. Copies of Single Issue Published Nearest to Filing Date
a.	Total No. Copies (Net press run)	4,000	3,700
b.	Paid and/or Requested Circulation		
	(1) Sales through dealers and carriers, street vendors, and counter sales (not mailed)	0	0
	(2) Paid or Requested Mail Subscriptions, (Including advertisers) proof copies and exchange copies)	3,804	3,455
c.	Total Paid and/or Requested Circulation (Sum of b (1) and b (2))	3,804	3,455
d.	Distribution by Mail (Samples, complimentary, and other free)	0	0
e.	Free Distribution Outside the Mail (Carriers or other means)	0	0
f.	Total Free Distribution (Sum of d and e)	0	0
g.	Total Distribution (Sum of c and f)	3,804	3,455
h.	Copies Not Distributed		
	(1) Office use, leftovers, spoiled	196	255
	(2) Returned from news agents	0	0
i.	Total (Sum of g, h (1), and h (2))	4,000	3,700
Percent Paid and/or Requested Circulation (c/g x 100)		100%	100%